EPRI | ELECTRIC POWER RESEARCH INSTITUTE

Delayed Hydride Cracking Considerations Relevant to Spent Nuclear Fuel Storage

2011 TECHNICAL REPORT

WARNING:
Please read the Export Control Agreement on the back cover.

Delayed Hydride Cracking Considerations Relevant to Spent Nuclear Fuel Storage

This document does NOT meet the requirements of 10CFR50 Appendix B, 10CFR Part 21, ANSI N45.2-1977 and/or the intent of ISO-9001 (1994)

EPRI Project Manager
A. Machiels

ELECTRIC POWER RESEARCH INSTITUTE

3420 Hillview Avenue
Palo Alto, CA 94304-1338
USA

PO Box 10412
Palo Alto, CA 94303-0813
USA

800.313.3774
650.855.2121

askepri@epri.com

www.epri.com

1022921
Final Report, July 2011

DISCLAIMER OF WARRANTIES AND LIMITATION OF LIABILITIES

The following organization, under contract to EPRI, prepared this report:

Tomari Consulting

NOTE

For further information about EPRI, call the EPRI Customer Assistance Center at 800.313.3774 or e-mail askepri@epri.com.

Acknowledgments

The following organization, under contract to the Electric Power Research Institute (EPRI), prepared this report:

Tomari Consulting
6 Ryan's Camp Lane, RR1
Deep River, Ontario
Canada K0J 1P0

Principal Investigator
C. E. Coleman

This report describes research sponsored by EPRI.

This publication is a corporate document that should be cited in the literature in the following manner:

Delayed Hydride Cracking Considerations Relevant to Spent Nuclear Fuel Storage
EPRI, Palo Alto, CA: 2011.
1022921

Abstract

In this report, the main features of delayed hydride cracking (DHC) in zirconium alloys are reviewed. The conditions inside fuel rods during **dry** storage are estimated and used to evaluate whether DHC is possible during dry storage. Although some of the conditions for DHC exist—sufficient hydrogen for hydride formation, cooling from a high temperature, and long times—crack initiation is unlikely because either the required high stresses or large sharp flaws are absent.

In addition, DHC in zirconium alloys at low temperatures is reviewed. The conditions inside fuel rods during **wet** storage are estimated and used to evaluate whether DHC is possible during pool storage. Crack initiation, and therefore crack growth, is unlikely because the tensile stresses are too low, even if the outside surface of the cladding contains fretting damage from grids of modern design. If cracks were nucleated, they would grow sufficiently quickly that they would be apparent during pool storage. Their absence supports the conclusion that DHC is improbable.

In several recent publications, Y. S. Kim has proposed a model for DHC, which is claimed to be new and superior to the model used in this study. The source of the disagreement is in the development of the first step—that is, crack initiation—of the process. The two basic mechanisms are reviewed and compared, and it is shown that Y. S. Kim is not justified in criticizing the model used in this study.

Keywords
Crack initiation
Crack propagation
Delayed hydrogen cracking
Dry storage
Spent fuel
Wet storage

Table of Contents

List of Figures

List of Tables

Section 1: Possibility of Delayed Hydride Cracking During Dry Storage of Spent Nuclear Fuel

1.1 Introduction

Once nuclear fuel has provided its energy and the absorption rate of neutrons approaches their production rate, the fuel is discharged from the reactor into pools of water, where it is stored for a minimum of five years. Subsequent storage in dry conditions, in containers called casks and silos, is less costly to implement compared to storage in water and is used in many countries [1]. Dry storage times for a century are envisaged. The environment for dry storage may be air or an inert gas, such as nitrogen or helium, depending on the expected cladding temperatures of spent fuel elements. Maintaining integrity of the cladding is desirable to minimise spread of radioactivity and ease further handling.

The decay of radioisotopes generates heat that is readily dispersed during residence in the pool, so these conditions are benign. During transport and dry storage in an inert gas, the temperature may rise to several hundred degrees Celsius and cladding stresses are provided by the pressure of the filler gas, usually He, released fission gases and He from transmutation of boron, sometimes present as a burnable poison. Once outside the reactor, further contributions to gas pressure from α-decay are very small, unless Pu isotopes are present. With time both temperature and stress decline and therefore the first period of dry storage is of most concern. EPRI has an interest in the possible ways zirconium alloy fuel cladding may fail under dry storage conditions after service in a Light Water Reactor (LWR). (Note that the burn-up in CANDU fuel is 4 to 10 times lower than in LWRs, consequently the temperatures at the start of dry storage are very low, often about 150 °C [2]. Stress-induced failures are not an issue because the initial gas pressure is around atmospheric pressure and the inventory of fission gasses is low. Spent fuels from these power reactors have been stored in air for many years with no problem.)

In an EPRI report issued in 2000 [3], the opinion was expressed that deformation by creep was the dominant deformation mechanism and could be accommodated while cracking mechanisms, such as stress corrosion cracking from fission products and Delayed Hydride Cracking (DHC) were unlikely to operate during dry storage. At the time there was said to be little or no evidence

for DHC in fuel cladding. In this Section, the conclusions reached in Chapter 3 of the 2000 report [3] are reviewed in the light of recent experimental results. DHC is separated into crack initiation and crack propagation. The temperature dependence and the way it is attained are important for application to fuel storage. Consistent with conclusions reached in Reference [3], the key to the application of the mechanism is initiation since propagation of a crack in fuel cladding by DHC will be shown to be a viable process at some time during dry storage.

The hydrogen concentration is taken as much elevated from the initial value. Hydrides can be the consequence of the presence of hydrogen in zirconium alloys because the solubility limits (i.e., Terminal Solid Solubility (TSS)) for hydrogen in zirconium are very low. There are two solubility limits, TSSD for dissolution on heating and TSSP for precipitation on cooling. They are described by the van't Hoff equation:

$$TSS = A \exp(-H/RT) \qquad \text{Equation 1-1}$$

where A = Constant
H = Solvus enthalpy
R = Gas constant
T = Temperature [K]

Typical values for TSSD are: $A_{TSSD} = 8.19 \times 10^4$ ppm and $H_{TSSD} = 34.5$ kJ/mol, and for TSSP: $A_{TSSP} = 4.11 \times 10^4$ ppm and $H_{TSSP} = 28$ kJ/mol [4]. Values plotted in Figure 1-1 show that hydrides dissolve 50 to 60 °C above the temperature at which they precipitate. At hydrogen concentrations > 1 ppm, hydrides will always be present at room temperature, while 5 ppm hydrogen is sufficient to produce hydrides at 100 °C. At 400 °C, 172 ppm hydrogen will dissolve in zirconium but the same material would have to be cooled to 342 °C before hydrides would precipitate.

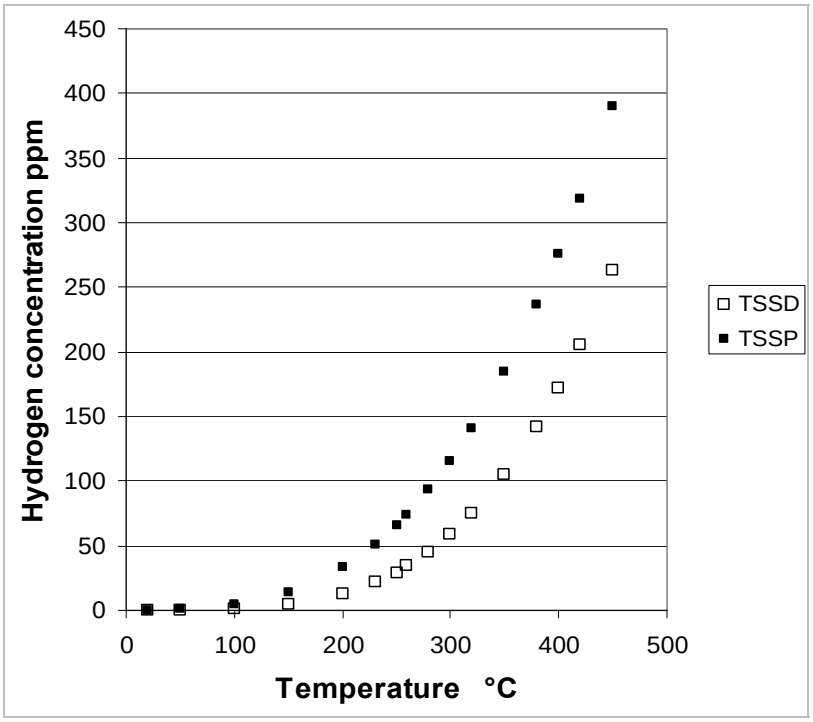

Figure 1-1
Solubility limits for hydrogen in zirconium: on heating (TSSD) and on cooling (TSSP) [4]

In several recent publications, Y.S. Kim [5] has proposed a model for the rate of DHC that is claimed to be new and superior to previous models. The source of the disagreement is in the development of the first step of the process. The two basic mechanisms will be reviewed and compared in Appendix A. It will be shown that Kim is not justified in criticizing the previous models.

1.2 Delayed Hydride Cracking (DHC)

DHC is a time-dependent mechanism of crack propagation in zirconium alloys. It involves the diffusion of hydrogen, but also the microscopic fracture of zirconium hydride, leading to the initiation and propagation of a macroscopic crack. Most of the data on DHC comes from experiments on Zr-2.5Nb, which therefore provides the most confidence in conclusions; the Zircaloys should behave qualitatively in the same manner. DHC has several characteristics.

- A threshold mechanical loading for crack initiation is required. If no flaw is present, the process can only start with very large tensile stresses; if a sharp flaw is present in the component, a threshold stress intensity factor, K_{IH}, has to be exceeded. Subsequent crack propagation rate, V, is almost independent of the applied stress intensity factor, K_I. Figure 1-2 describes this behavior.

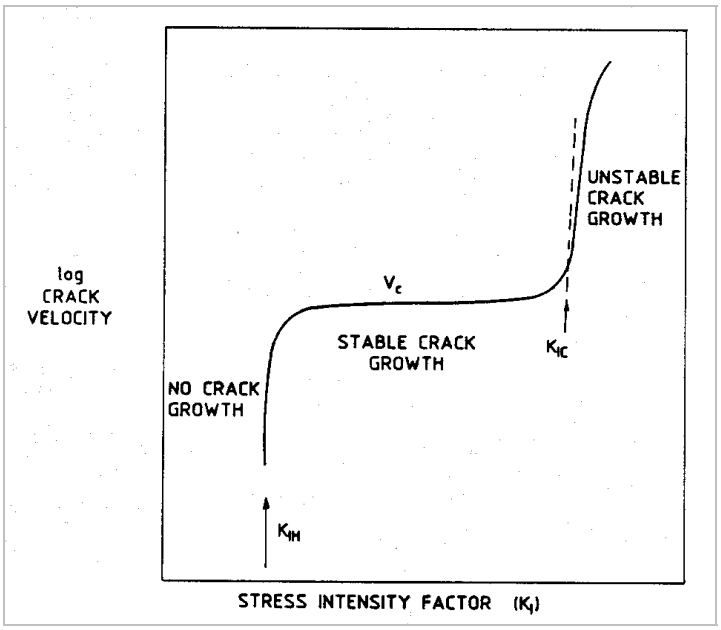

Figure 1-2
Dependence of DHC rate on stress intensity factor, K_I.

- In Zr-2.5Nb cracking has been observed in components containing residual tensile stresses, produced by mechanical work in pressure tubes [6] or by welding [7, 8]. The damaging residual stresses were up to 600 MPa; the reference limit stress for crack initiation from a smooth surface is 450 MPa based on tests using temperature cycling [4].
- The values of K_{IH} from experiments are variable and often less than 10 MPa√m; the reference lower bound for Zr-2.5Nb pressure tubes is 4.5 MPa√m [4]. Up to some high temperature, K_{IH} is not very sensitive to temperature. As an example, in one experiment on Zr-2.5Nb, K_{IH} remained around 8 MPa√m up to about 300 ºC, but increased rapidly at higher temperatures, Figure 1-3 [9].

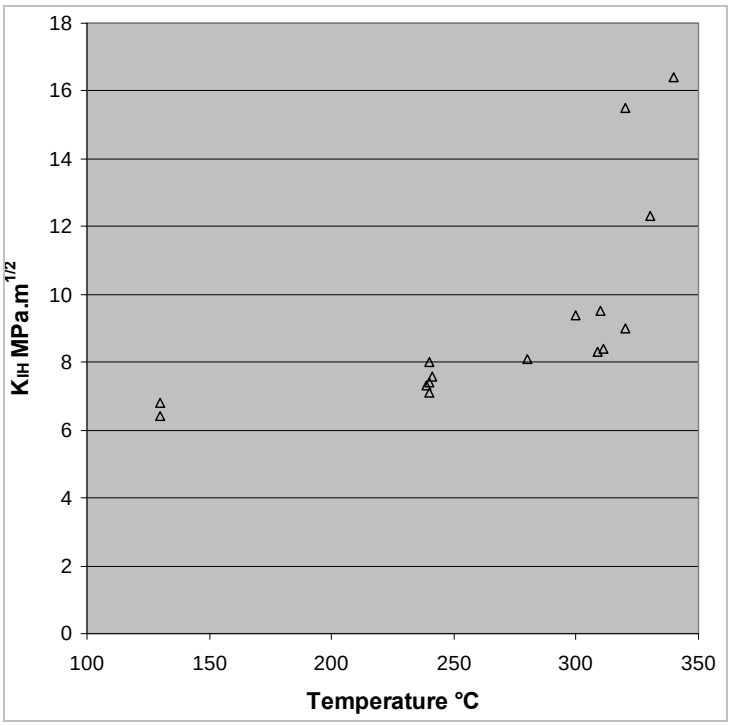

Figure 1-3
Abrupt change in temperature dependence of K_{IH} above 300 °C in irradiated Zr-2.5Nb pressure tube material containing 153 ppm of hydrogen [9]

- K_{IH} is not very sensitive to material strength. For example, in Zr-2.5Nb, while neutron irradiation increases the yield strength by 200 to 300 MPa, irradiation causes only a small reduction in K_{IH} in Zr-2.5Nb, Figure 1-4 [10].

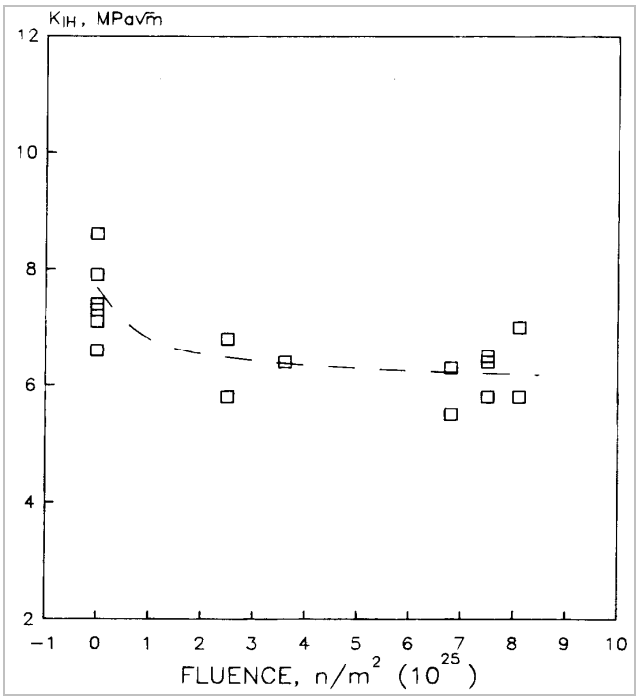

Figure 1-4
Effect of neutron irradiation on K_{IH} of cold-worked Zr-2.5Nb at 140 °C [10]

- V is very sensitive to temperature and temperature history. Often V is described by an Arrhenius equation:

$$V = C \exp(-E/RT) \qquad \text{Equation 1-2}$$

where C = Constant
E = Apparent activation energy for cracking,
R = Gas constant
T = Temperature [K]

- The importance of temperature history is shown schematically in Figure 1-5 [11]. As the temperature is raised from T_1, cracking velocity follows Equation 1-2 until a temperature is reached where the cracking rate starts to decline, T_2, and eventually stops (i.e., V = 0) at a slightly higher temperature, T_3, even if hydrides are present in the component. In another history, upon cooling from some high temperature, T_4, a temperature is reached where cracking starts, T_5, and upon additional cooling, the velocity reaches a maximum value at T_6. This cracking can happen even if all the hydrogen is in solid solution and no hydrides are present in the bulk of the component. Cracking at subsequent lower temperatures again follows Equation 1-2. Typical maximum velocities are 9×10^{-8} m/s at 250 °C and 5×10^{-9} m/s at 150 °C in cold-worked Zr-2.5Nb.

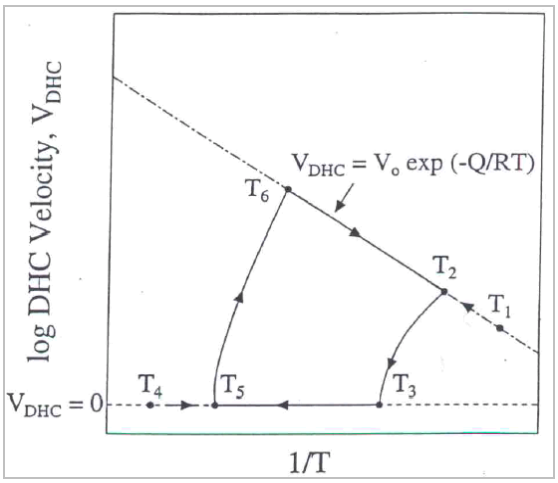

Figure 1-5
Schematic diagram of the effect of temperature history on DHC rate [11]

- A positive temperature gradient (i.e., the crack tip being cooler than the metal matrix) increases V and shifts T_2 and T_3 to higher values [12], Figure 1-6. For example, a gradient of 20 °C/mm increases V by a factor of 2.6 and shifts T_3 by 150 °C. T_5 and T_6 have not been evaluated, but they too should be shifted to higher values.

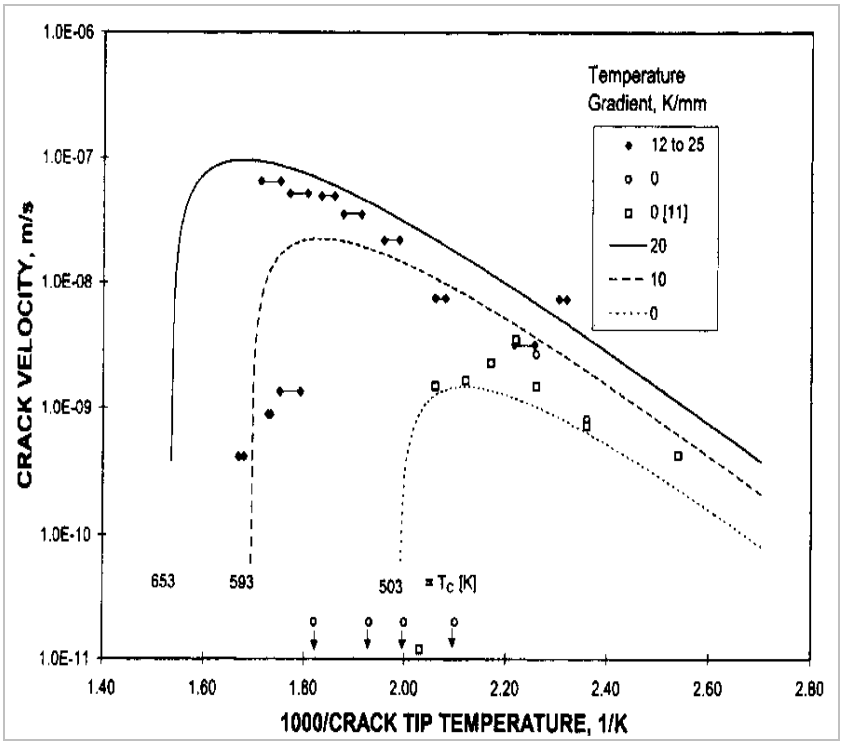

Figure 1-6
Delayed hydride cracking after heating to test temperature, showing rise in T_2 and T_3 with increase in positive temperature gradient [12]

- A high temperature exists above which DHC is absent, T_0, despite having hydrides present and cooling to the temperature [13]. Figure 1-7 illustrates this phenomenon in Zr-2.5Nb containing 170 ppm hydrogen. In this example, no DHC was observed above 350 ˚C. The rise in K_{IH} with temperature above 300 ˚C, Figure 1-3, is partially responsible for this behavior. Irradiation increases T_0; for example, T_0 is increased to over 365 ˚C in Zr-2.5Nb by a neutron fluence of 3.5 x 10^{25} n/m^2, E > 1 MeV.

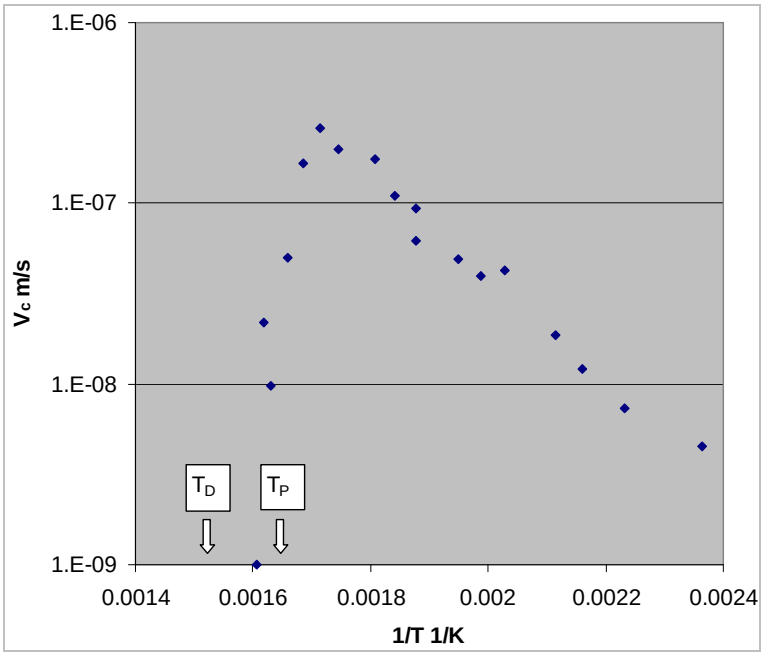

Figure 1-7
Evaluation of high temperature limit in Zr-2.5Nb containing 170 ppm hydrogen with test temperature attained by cooling. Decline in V_c starts at temperatures below the solubility limit for hydride precipitation, T_P, that is, hydrides were present (based on data in [9])

- An increase in strength raises V. In Zr-2.5Nb neutron irradiation often adds 200 to 300 MPa to the yield strength resulting in V being increased by a factor of ten [10, 14].

In summary, the main parameters of DHC and their dependence on temperature and load have been established for Zr-2.5Nb.

1.3 DHC in Zircaloy and Fuel Cladding

Failures of fuel rods by DHC are less clear than in components made from Zr-2.5Nb, for example, pressure tubes [6], because of complicating factors in fuel cladding such as oxidation of the fracture surface and DHC being the propagating mechanism rather than the primary cause of the cracking. At first sight, Zircaloy[1] would seem to be less susceptible to DHC than Zr-2.5Nb; the

[1] For DHC, Zircaloy-2, Zircaloy-4 and their variants can be considered as the same material and will be called “Zircaloy”.

strength is lower and the microstructure is single phase, except for a small volume fraction of intermetallic particles, whereas Zr-2.5Nb is often prepared with the α-phase surrounded by the β-phase. The diffusivity of hydrogen is smaller in the α-phase than in the β-phase and the latter acts as an easy pathway for the diffusion of hydrogen. Fewer experiments have been done on Zircaloy than on Zr-2.5Nb, but its DHC behavior can be clearly discerned.

Laboratory measurements on Zircaloy confirm that V is lower than in Zr-2.5Nb. For example, Figure 1-8 compares values obtained from unirradiated, cold-worked and stress-relieved Zr-2.5Nb pressure tube material containing up to 72 ppm hydrogen [15] and unirradiated, cold-worked and stress-relieved Zircaloy fuel cladding containing 200 ppm hydrogen [16]; the velocity values for Zircaloy are two to three times lower than in Zr-2.5Nb, but the temperature dependencies are similar. Other values from pressure tubes [17, 18] and fuel cladding [19, 20] made from Zircaloy, Figure 1-9, are in general agreement with the values shown in Figure 1-8.

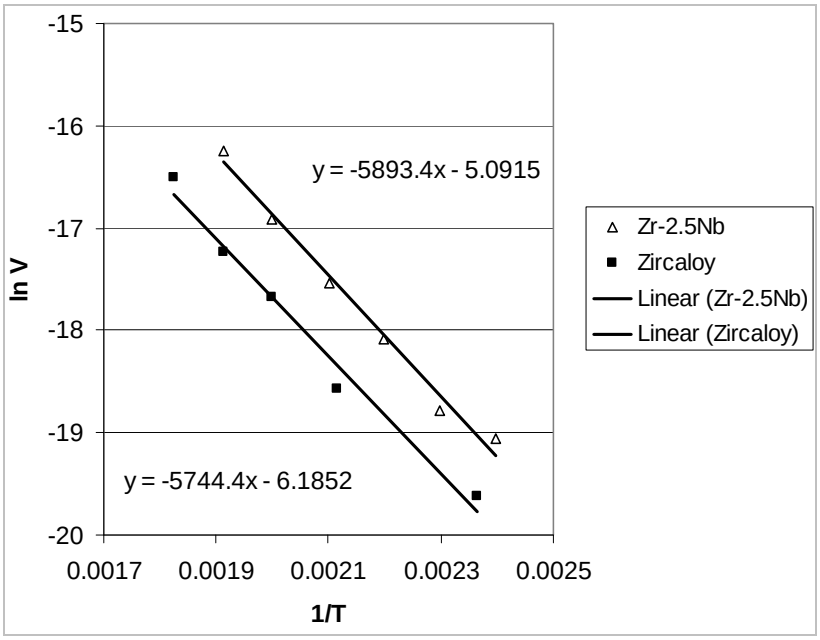

Figure 1-8
Comparison of DHC velocity in Zr-2.5Nb and Zircaloy in similar metallurgical conditions (based on data in [15] and [16])

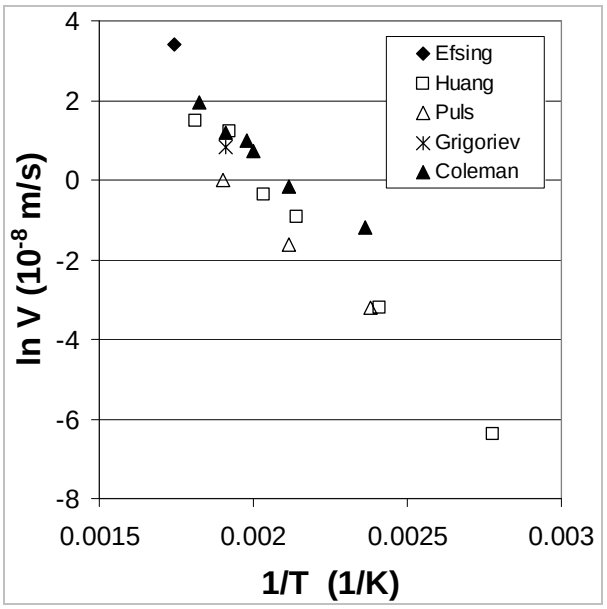

Figure 1-9
Temperature dependence of V in Zircaloy (data from [16 to 20])

Neutron irradiation increases V in Zircaloy; in pressure tube material, an increase of nearly thirty-times was observed [18] while in fuel cladding the increase was between three and ten times [20, 21]. In irradiated Zircaloy, the values of T_3 and T_5 are similar to those observed in Zr-2.5Nb [22]. A high temperature limit, T_0, of around 290 ºC has been observed in unirradiated Zircaloy cladding containing 200 ppm hydrogen [16], Figure 1-10. A value of T_0 around 360 ºC has been observed in irradiated Zircaloy cladding [23].

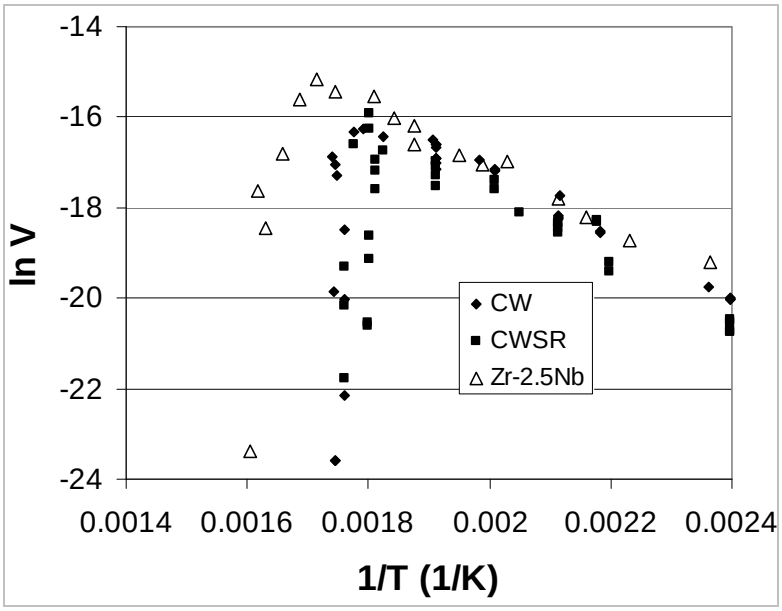

Figure 1-10
Reduction in DHC at high temperatures in Zr-2.5Nb and CW and CWSR Zircaloy fuel cladding (based on [9, 16])

A radial temperature gradient can augment DHC on Zircaloy fuel cladding [24], even when the temperature is attained by heating. With modest hydrogen concentrations, 100 to 120 ppm, at a cracking temperature of 250 °C, cracking was increased by two to three times by a temperature gradient of about 60 °C /mm. At 275 °C, DHC was only observed when the temperature gradient was present. No cracking was obtained at 288 °C with or without a temperature gradient. An increase of hydrogen concentration to 352 ppm combined with the temperature gradient induced cracking at a crack tip temperature of 288 °C, but none in the absence of the gradient. These results are in concordance with the theory presented in Figure 1-6. They also show easy cracking at a crack tip temperature that is above T_0 indicated in Figure 1-10.

As with Zr-2.5Nb, values of K_{IH} of 10 MPa√m or less have been reported for Zircaloy pressure tubes and fuel cladding, as summarized in Table 1-1. Although there is much scatter, the small effect of irradiation on K_{IH} is indicated.

Table 1-1
Values of K_{IH} for Zircaloy

Material	Irradiated?	Test temperature [°C]	Hydrogen concentration [ppm]	K_{IH} [MPa√m]	Reference
Pressure tube	No	150 to 200	180 to 300	7 to 8	[18]
Pressure tube	Yes	150 to 200	180	6	[18]
Pressure tube	No	Cycle to 250	40	5	[11]
Fuel cladding - RXA	Yes	250 to 300	Up to 350	6 to 11	[20]
Fuel cladding - CWSR	No	300	1000	6 to 8	[19]
Fuel cladding - RXA	No	300	500	14	[19]
Fuel cladding - LK-2	Yes	200 to 300	560 to 1900	9.9 to 12.7	[21]

Some cracks in fuel cladding in LWRs have been attributed to DHC or a DHC-like process:

- Secondary cracking leading to long slits in BWRs was caused by the production of copious amounts of hydrogen inside the fuel rod from a process called 'oxygen starvation' [25, 26]. The fracture surfaces looked similar to those produced by a DHC-like mechanism and the crack velocities at about 270 ºC were in the range of 2 to 7 x 10^{-7} m/s, expected for DHC in irradiated cladding [26]. The exact mechanism of cracking is still under discussion and DHC is not entirely precluded.
- Radial cracking from the outside surface, again with fracture features similar to DHC, has been observed in power ramp tests after burnups of 40 to 60 GWd/t in a commercial BWR [27]. Subsequent laboratory tests simulating the loading conditions showed that the cracking had the properties of DHC [28]. Care has to be taken with these results because the in-reactor test conditions were outside the operating range of BWRs. These conditions of a relatively cold crack tip, a large temperature gradient and a large force from the power ramp were ideal for the DHC process.
- 20-mm long cracks in the axial direction, close to the end-plugs of CANDU fuel have been detected [29]. The burn-up was very low, 0.4 GWd/t, so the inventory of fission products would be too small to cause stress-corrosion

cracking. Several partial radial cracks had also started from the inside surface. The hydrogen concentration was 42 ppm, which may have been picked up from residual moisture in the fuel. The source of the large hoop stress driving the crack was attributed to fuel expansion from the fuel operating well outside its design power, although the cause of this anomaly was not identified.

In summary, fuel cladding made from Zircaloy is not immune from DHC and can behave similarly to Zr-2.5Nb. In-reactor failures have only been observed in fuel that is operating well outside its design limits.

1.4 Condition of Fuel Cladding after Service

Three factors are important for DHC during handling and storage of fuel: mechanical properties, hydrogen concentration and mechanical damage.

1.4.1 Mechanical Properties

The increase in yield strength as a function of the irradiation dose for stress-relieved and recrystallized Zircaloy-2 and Zircaloy-4 has been reviewed for a large number of irradiation conditions [30]. After a rapid rise in strength with low dose, the subsequent increase in strength is smaller with higher neutron fluence leading to a saturation mechanism, both with low temperature irradiation and when the irradiation is performed in the range of 250 to 300 °C. For recrystallized alloys, the irradiation can induce a twofold increase of the yield strength. For cold-worked and stress-relieved materials, having a higher strength before irradiation, the relative increase in yield strength is smaller. The two conditions will exhibit similar yield strengths after an irradiation dose of about 10^{25} n/m^2, at which the irradiation hardening tends to saturate. Later observations have not changed these conclusions.

In addition to the increase in yield strength, a large decrease in ductility, as measured by elongation, is induced by irradiation. This reduction in elongation is linked to the localisation of the deformation in narrow bands that produces a strong decrease in strain hardening. Plastic elongation below 1 % can be observed for Zr alloy fuel cladding, after less than one cycle of irradiation in power reactors [31, 32]. This low elongation is not an embrittlement (such as cleavage or intergranular fracture), but a change in the mechanism of deformation. The fracture surfaces remain characteristic of local ductile behavior, with dimples and the absence of any traces of cleavage. The reduction in strain to failure is caused by a large reduction of the uniform strain from highly localised deformation.

During storage, the temperature of the cladding can be higher than the temperature during irradiation. As with any heat-treatment performed in alloys whose microstructures are not in equilibrium, a recovery process can be observed in irradiated zirconium alloys when the post-irradiation temperature is higher than the irradiation temperature. The experimental studies have mostly focussed on the kinetics of recovery of the irradiation damage at temperatures much higher than the temperature of irradiation. All the studies are in agreement and

converge for a beginning of the recovery around the irradiation temperature and total recovery at 550 ºC within 200 s (for example, [33]). Cladding irradiated up to $1x10^{26}$ n/m^2 between 320 to 350 ºC in a PWR and annealed at 350 ºC lost most of its irradiation hardening after 3000 h. This thermal recovery was not affected by a stress of 130 MPa [34].

1.4.2 Hydrogen Pick up

During residence in a power reactor, fuel cladding picks up hydrogen released during corrosion. At fuel burn-ups of 50 GWd/t or greater in BWRs, the hydrogen concentration is often between 100 and 200 ppm [35, 36], but in one extreme case, was as high as 1600 ppm [37]. Compared with BWRs, fuel cladding picks up much more hydrogen in PWRs. As one example, after a fuel burn-up of about 57 GWd/t, low-tin Zircaloy-4 contained between 600 and 820 ppm of hydrogen [38].

The distribution of the hydrogen, and subsequent hydrides, is relevant for DHC.

- Upon dissolution and reprecipitation, hydrides can be reoriented by a tensile stress. In a tube a desirable orientation of hydride platelets is with their normal in the radial direction; such hydrides are called circumferential hydrides. Circumferential hydrides, even at very high concentrations, have little effect on tensile ductility [39, 40]. Cooling the tube under a hoop stress from a temperature where much of the hydrogen is in solution may result in hydrides precipitating with their normal in the circumferential direction; these hydrides are called radial hydrides. Radial hydrides may severely embrittle the tube [41]. A threshold stress is required to form radial hydrides. Typical values are 120 MPa for cold-worked, stress-relieved (CWSR) cladding and 70 MPa for recrystallized, annealed (RXA) cladding [42].
- The ability to form radial hydrides may also be important for DHC. For example, Zr-2.5Nb pressure tubes crack readily with a hoop stress, because radial hydrides form at the crack tip, whereas with a longitudinal stress cracking is difficult because the distribution of hydrides at the crack tip is very diffuse. The explanation of this behavior is based on the texture of the material, which consists of a large texture factor for basal normals in the transverse direction and a small one in the longitudinal direction [43].
- The inside of the fuel cladding is much hotter than the outside and hydrogen diffuses down the temperature gradient towards the outer regions of the cladding [44]. The subsequent layer with a high density of hydrides coupled with a thick oxide on the outside surface may be the source of crack initiation [45].

1.4.3 Mechanical Damage

Unless tensile stresses are very large in a component, a stress raiser is required to initiate DHC. Flaws may be produced during operation, for example by stress-corrosion from fission products on the cladding inner surface or by fretting on the outer surface caused by vibration and contact with spacers, or during handling, causing scratches and gouges.

Thus before fuel is placed in storage, the cladding can have a wide range of irradiation damage, hydrogen concentration and distribution of subsequent hydrides, and perhaps some potential crack initiation sites.

1.5 Conditions during Fuel Storage

The conditions for dry storage are quite different from those during residence in the reactor, for which the fuel was designed. These differences include:

- Very long residence times, with targets of 40 to 100 years;
- No irradiation damage from neutrons;
- The external fluid, usually an inert gas such as helium, with heat-transfer that is less efficient than in water;
- Heating from radioactive decay that declines with time; because of the relatively poor heat-transfer the cladding temperature is raised from ambient temperatures by several hundreds of degrees Celsius, but because the heat flux is about 1 % of that during residence in the reactor, the temperature gradient through the cladding wall is very low, <1 °C/mm [46].
- The internal gas pressure from the original filler gas and fission products is greater than the ambient pressure – i.e., atmospheric pressure – leading to tensile hoop stresses.

The temperature is highest at the start of storage; consequently the pressure and the hoop stresses are highest then too. As the temperature is reduced, then the pressure decreases. If the cladding creeps, the pressure also decreases because of the extra volume.

The initial conditions for dry storage will depend on:

- The fuel composition: for example, in MOX fuel, α-decay leads to the generation of He, amounts of which can be large after very long storage times, > 100 years [47]; low diffusivity of He in ceramic fuel may postpone its release at fuel storage temperatures.
- The strength of the cladding: during reactor operation, weaker cladding creeps down and contacts the fuel earlier than strong cladding, resulting in a lower fuel temperature and less fission gas release and thus lower pressure at the start of dry storage after the same burnup.
- Fuel burn-up: higher values result in more decay heat and fission gases.
- Residence time in pool storage: longer times allow for greater cooling.

To prevent excess creep and potential rupture, regulators have set limits on the normal conditions of storage. For example, the US NRC has decreed that cladding temperature must not exceed 400 °C [48]. Cladding stresses have to be based on the cladding thickness reduced by any hydride layer and the thickness of the oxide; the maximum corrosion allowance is 120 μm, corresponding to a metal loss of 80 μm (120/1.5 μm, where 1.5 is the Pilling-Bedworth ratio.) One of the operating limits for PWR fuel is for the internal gas pressure to be lower than the

coolant water pressure, 15.5 MPa at 350 ºC. An upper-bound stress at the start of storage can be estimated using these values. At the limiting temperature of 400 ºC the internal pressure is raised to 16.7 MPa. In typical cladding the outside diameter is 9.5 mm and the wall thickness is 0.57 mm; the thickness is reduced to 0.49 mm by corrosion. The upper-bound hoop stress at 400 ºC is therefore about 150 MPa (based on PD/2t or 16.7x8.85/2x0.49). German regulators limit the hoop stress to 120 MPa, while in France the stress limit may be as high as 300 MPa, based on creep rupture behavior [49]. During loading of the fuel, not more than ten thermal cycles of less than 65 ºC are allowed; peak cladding temperature limits and thermal cycle restrictions are designed to minimize re-orienting hydrides to a radial configuration.

Calculation is used to determine the conditions for fuel storage. For example, at the start of dry storage after a burnup of 55 GWd/t and about 6 years in pool storage, typical predicted temperatures were 350 to 360 ºC declining to 230 to 240 ºC in ten years, according to [50]. The calculated hoop stresses at the start of storage were 60 to 80 MPa, which declined, from both the drop in temperature and less than 1 % creep strain, to 45 to 60 MPa, respectively [50]. In reference [51], similar calculations using the regulatory limit of 400 ºC were performed. The end-of-life internal pressure was used to calculate the hoop stress at the start of storage, using, for illustration, a maximum value as high as 200 MPa. The temperature and stress decline are illustrated in Figure 1-11 for an initial hoop stress of 100 MPa. After 40 years the temperature is predicted to be about 222 ºC while the stress has decreased to 68 MPa.

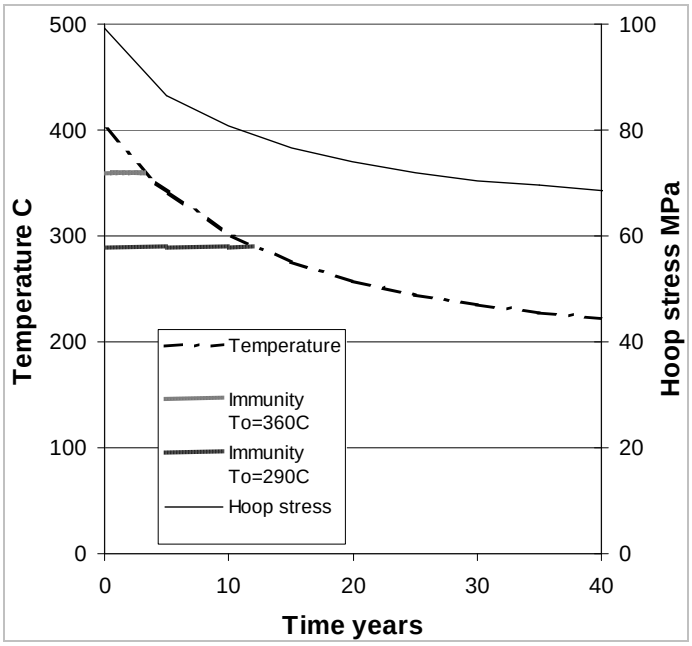

Figure 1-11
History of temperature and hoop stress imposed on fuel cladding during dry storage (based on [51]). Periods of immunity based on T_o

Examinations of fuel rods after storage confirm this picture and provide insight in what to expect from the behavior of the cladding. As an example, PWR fuel was stored in a dry, inert atmosphere for 14.8 years after a discharge burn-up of 35.7 GWd/t, and then destructively examined [52]. After some thermal benchmark tests, in which the maximum temperature reached 415 °C, but for less than 72 h, the fuel rods were stored in a Castor cask. The temperature at the start of dry storage was 344 °C; this temperature had declined to about 155 °C after 14.2 years. The contribution to the internal pressure from fission gases was 0.75 MPa for a total pressure of 3.61 MPa. No extra fission gas was released during storage. At 415 °C, this pressure would impose a hoop stress of 72 MPa, but at the start of dry storage (344 °C) this value would be 64 MPa. The maximum hydrogen concentration in the cladding was 325 ppm, consistent with PWR cladding at this burnup. It was either distributed evenly across the cladding wall or in concentrated bands on both the outer and inner regions of the cladding. No radial hydrides were observed. The maximum oxide thickness on the outside surface was 45 μm with no radial cracks in the micrographs presented in the paper. Hardness measurements indicated that some irradiation damage had recovered, but was thought to have happened mainly during the initial benchmark testing with little further recovery during long-term storage. No breaches in the integrity of the cladding were detected.

Similar results were obtained after a burn-up of 58 GWd/t in a PWR and storage for 20 years in air [53]. No prior storage in water is mentioned, nor are the initial and final temperatures reported. The fuel cladding was intact. The total internal gas pressure was 4.58 MPa; no extra fission gas was released during storage. If the highest temperature met the NRC temperature limit of 400 °C at the start of dry storage, the maximum hoop tensile stress would have been about 88 MPa. The maximum hydrogen concentration was 122 ppm. No hydride reorientation to radial hydrides was observed. Hydrogen would all be in solution for the first period of storage (about the first ten years, Figure 1-11) and by then the hoop tensile stress would have been close to or below the threshold stress for hydride reorientation.

In summary, during dry storage fuel cladding is subject to temperatures higher than during reactor operation and has to withstand a hoop tensile stress from the internal gas pressure since the water pressure during reactor operation is absent. Both temperature and stress decline slowly with time.

1.6 Is DHC Possible during Fuel Storage?

The critical conditions for DHC are for the material to be susceptible to DHC, for K_{IH} to be exceeded so that DHC can initiate, and for sufficient hydrogen to be present so that hydrides can form to allow the crack to propagate. This latter condition depends on the hydrogen concentration, the temperature and whether this temperature was attained by cooling or heating.

Much evidence has been accumulated showing that Zircaloy fuel cladding is susceptible to DHC and, if the correct conditions exist, can crack by DHC. Although the loading is mostly in plane stress, a stress gradient is setup at any

flaw, which is sufficient to induce hydrogen migration to the flaw tip. Even with favorable stressing conditions, a maximum temperature, T_0, exists above which DHC cannot start. This temperature is around 290 ºC in unirradiated cladding material but may be as high as 360 ºC in irradiated material. This phenomenon suggests that fuel that would start storage at the NRC-stipulated maximum temperature of 400 ºC will be immune from DHC until the temperature reaches the critical temperature. This period of immunity is about three years, using the cooling curve of Figure 1-11. If T_0 depends on irradiation damage, its value may be reduced if the damage is annealed out during early storage. Thus the period of immunity may be much longer than estimated; if T_0 returns to 290 ºC, the period of immunity increases to about 12 years, Figure 1-11. The hoop stress will be simultaneously lowered, providing further protection. The benefits from these arguments are smaller when the starting temperature for storage is lower than the NRC limit, as is generally the case, since the irradiation damage will be retained for longer times. Once the period of absolute immunity is over, one then has to examine the stress conditions.

After service in a power reactor, fuel cladding often contains much hydrogen so that hydrides are present throughout the period of storage. The discussion in Section 1.1 suggests that at the NRC maximum temperature, hydrides would still be present on heating if the concentration of hydrogen were 172 ppm. Below T_0, cracks only extend by DHC if the temperature is attained by cooling from some critically higher temperature, often TSSD. In much of the fuel cladding removed from LWRs, DHC would not be limited by lack of hydrogen.

The unfavorable effects of a temperature gradient, described in Section 1-2, are mostly absent during fuel storage. Once dry storage has begun, the cladding is slowly cooled, which strongly favors DHC. Thus the conditions for crack propagation will be present at some time during fuel storage.

For a crack to be initiated, the combination of tensile stress and flaw size must exceed K_{IH}. (Although K_{IH} is a linear elastic concept it can be used as a guide for this discussion because its measurements were made on fuel cladding.) The maximum depth of sharp surface flaw, a, that can be tolerated without crack growth can be estimated from [54]:

$$a = (K_{IH}/\sigma)^2 \, Q/(1.2\,\pi) \qquad \text{Equation 1-3}$$

where σ = Applied stress
Q = Shape factor

For elliptical flaws, Q is about 1.5 while for long flaws, for example, a scratch, Q is about 1.0. Applying the information from this review indicates that the flaws have to be unrealistically large (deeper than the thickness of the cladding) or the stress has to be at one of the maximum estimated values cited above, which are probably unrealistically large, Table 1-2. These conditions suggest that the flaws would be detected before the fuel was placed in storage or deformation and plastic collapse would intervene before DHC could start. Thus crack initiation by DHC is a highly unlikely event. If K_{IH} increases to much higher values above

300 ºC, as indicated for irradiated Zr-2.5Nb, then this conclusion is further reinforced.

Table 1-2
Critical flaw depth for crack initiation by DHC (wall thickness taken as 0.57 mm)

Crack shape depth/length	Q/(1.21 π)	K_{IH} [MPa$\sqrt{m}$[	Tensile stress [MPa]	Flaw depth [mm]	Flaw depth/Wall thickness
0.3	0.39	5	90	1.20	2.14
0.3	0.39	5	120	0.69	1.20
0.3	0.39	5	150	0.43	0.77
0.3	0.39	5	200	0.24	0.43
0.3	0.39	10	90	4.81	8.55
0.3	0.39	10	120	2.74	4.81
0.3	0.39	10	150	1.73	3.08
0.3	0.39	10	200	0.98	1.73
< 0.1	0.26	5	90	0.80	1.42
< 0.1	0.26	5	120	0.46	0.80
< 0.1	0.26	5	150	0.29	0.51
< 0.1	0.26	5	200	0.16	0.29
< 0.1	0.26	10	90	3.21	5.70
< 0.1	0.26	10	120	1.83	3.20
< 0.1	0.26	10	150	1.16	2.05
< 0.1	0.26	10	200	0.65	1.15

Note that Chapter 3 of Ref. [3] came to similar conclusions about DHC initiation and propagation, but from a slightly different direction.

1.7 Summary and Conclusions

The main features of delayed hydride crack in zirconium alloys and the conditions for dry storage of spent nuclear fuel are summarized. Although at some time during storage the conditions for DHC propagation will be present, starting such a crack would require unacceptable tensile stresses or unrealistic sharp flaws.

1.8 Recommendations

Confirmation of three quantities would reinforce the conclusion.

1. The value of K_{IH} for irradiated fuel cladding, especially above 300 ºC, needs to be measured.

2. The value of T_0 should be confirmed for irradiated fuel cladding since it is potentially a source of much margin on any cracking during dry storage.
3. Evaluation of the annealing of irradiation damage at temperatures a few tens of degrees Celsius above the irradiation temperature.

Section 2: Possibility of Delayed Hydride Cracking During Wet Storage of Spent Nuclear Fuel

2.1 Introduction

Before fuel from Light Water Reactors (LWR) can be stored in dry systems, the initial intense decay heat is dispersed in water held in large pools. Pool storage lasts at least five years or more, depending on the burnup of the fuel. The ambient conditions in a pool are benign, with low temperatures and small pressures from the head of water in the pool. The conditions inside the fuel rods and the metallurgical state of the cladding, including damage sustained during service, need to be assessed so that the transfer from the pool to, and storage in, dry conditions can be done safely. In Section 1, the prospects for leakage of radioactivity from the fuel during dry storage, because of a breach caused by DHC, was discussed and shown to be unlikely. In this Section, this information is used to evaluate the conditions during pool storage with an emphasis on fretting damage and the cladding conditions on entry into dry storage.

DHC at low temperatures is reviewed, an estimate of the conditions within the cladding and fretting damage are discussed and an assessment of DHC is made. In particular, assuming DHC at the fretting location during pool storage, how long would be required to penetrate the fuel cladding? Also, what would be the domain of conditions for DHC not to be active in the pool, but becoming active upon transfer of the PWR spent fuel assemblies?

2.2 DHC at Low Temperatures

DHC requires hydrogen to move to a stress-concentration and for the hydrogen concentration to exceed the solubility limit and form hydrides. If the local stress is large enough, these hydrides will fracture and the process will repeat and cracking will have started. The two technological parameters of interest are the rate of crack growth, V, and some measure of the critical stress needed to start the process. Usually the latter is identified as K_{IH}, the critical stress intensity factor, but it requires that the flaw is sharp. With blunt flaws or smooth surfaces, a critical tensile stress is required.

Measurements of V are important for evaluations of Leak-Before-Break in pressure tubes [55] and to determine times to breach fuel cladding if DHC can be initiated. Most measurements are made with cracks growing on the plane with its normal parallel with the hoop direction. The few measurements of V made below about 100 °C fit with the majority of the data obtained at higher temperatures. Table 2-1 summarizes the test data for pressure tubes made from Zircaloy-2 [18] and Zr-2.5Nb [56, 57, 58]. The microstructure of Zr-2.5Nb is highly anisotropic with α-grains in the shape of platelets, surrounded by β-phase; the normal to the α-grains is in the radial direction. It is this microstructural anisotropy that is thought to be responsible for the difference in V in the two test directions on the plane normal to the hoop direction, with cracking being more difficult in the radial direction. Similar anisotropy is less or absent in Zircaloy [18] because the microstructure is relatively more equiaxed. For cladding, one has to extrapolate values from above 150 °C [16, 59]. As with pressure tube materials, above about 200 °C, the rate of crack growth was similar in the radial and axial directions on the plane normal to the hoop direction [28, 59], Figure 2-1. In both pressure tube materials, DHC is very difficult when the crack is being driven by an axial stress; K_{IH} is 15 MPa√m, or greater [43]. This resistance to cracking is attributed to the lack of basal plane normals, and therefore normals to the habit planes of the hydrides, in the axial direction [18, 43]. Similar tests have not been performed on fuel cladding, but the lack of basal poles in the axial direction suggests it should behave similarly and be very resistant to DHC driven by an axial stress.

Table 2-1
DHC growth rates at low temperatures in zirconium alloys

Material	Test direction	Test temperature [°C]	V [m/s]	Reference
Zr-2.5Nb pressure tube	Axial	108	2.5×10^{-9}	[58]
Zr-2.5Nb pressure tube	Radial	77	7.7×10^{-11}	[56]
Zr-2.5Nb pressure tube	Radial	17	5.3×10^{-12}	[56]
Zr-2.5Nb pressure tube	Axial	20	3×10^{-10}	[57]
Zircaloy-2 pressure tube	Axial	93	5×10^{-10}	[18]
Zircaloy-4 fuel cladding	Axial Radial	100	4.3×10^{-10}	Extrapolated values [16, 28, 59]
Zircaloy-4 fuel cladding	Axial Radial	40	2.3×10^{-11}	Extrapolated values [16, 28, 59]

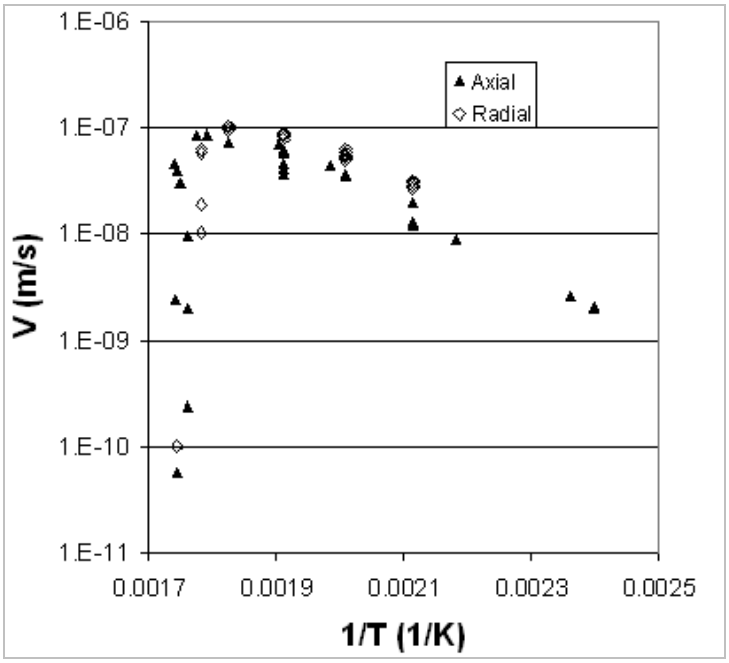

Figure 2-1
Comparison of temperature dependence of cracking in axial and radial directions in CWSR Zircaloy-4 fuel cladding [28, 59]

The crack growth rates above 100 °C are increased by neutron irradiation by factors between three and ten [10, 18, 20, 21], but no data exist below 100 °C. One rolled joint from a CANDU reactor containing a cracked Zr-2.5Nb pressure tube was held in a storage pool at about 20 °C for about 20 years and examined. The crack had extended axially, being driven by the original residual stresses that caused the crack in the first place. The average crack growth rate was about $2x10^{-11}$ m/s [60]. Unfortunately for this exercise, the fluence was very low in this region, so little effect of irradiation would be expected.

Values of K_{IH} are not sensitive to temperature below about 300 °C. The summary Table 1-1 provided in Section 1 should apply to temperatures below 100 °C. As in Section 1, the lower bound value of K_{IH} is taken as 5 MPa√m. In Zr-2.5Nb, the stress required to initiate DHC on a smooth surface is 450 MPa [4] and in the absence of any other information the same value will be used for irradiated Zircaloy fuel cladding.

2.3 Condition of a Fuel Rod

For this assessment the temperature of the pool water will be taken as 40 °C. Since the coefficient in thermal expansion of UO_2 [61] is over 60% larger than that of the diametral change in the cladding [62] (assuming a radial texture), on cooling from service conditions to pool conditions the fuel will shrink away from the cladding and will only be in loose contact with the cladding. Thus the main stressing agent will be internal pressure from the gasses. As in Section 1, the

internal pressure is assumed to be that based on the operating limits for PWR fuel in which the internal gas pressure has to be lower than the coolant water pressure, 15.5 MPa at 350 ºC. Taking account of the corrosion allowance, the maximum hoop stress at 40 ºC will be 70 MPa. Although there will be some heat flux, the temperature gradient will be small enough to ignore.

The cladding will be irradiation hardened and contain much hydrogen from corrosion. At 40 ˚C the solubility of hydrogen in zirconium alloys is less than 1 ppm so most of the hydrogen will be present as hydride [4]. As a result of the low hoop stress and low concentration of hydrogen in solution, the population of any radial hydrides will not increase during residence in a water pool.

Fretting can damage the outer surface of the cladding. Fretting from debris can be random and highly damaging, but for this report it is assumed that filters have kept such damage under control.

In Pressurized Water Reactors (PWR), the most likely damage is wear at the support locations between the fuel rod cladding and spacer grids, where the fuel rods are initially pre-loaded using an arrangement of springs and dimples. Failures of cladding from these interactions have been summarized in [63], indicating that fretting damage can penetrate the tube wall. For this report, potential damage in assemblies designed to mitigate fretting will be used for an example [64]. A schematic diagram of the fuel grid support is shown in Figure 2-2. The grid supports are usually made from Zircaloy-4 or other optimized zirconium alloys. During service, the spring relaxes, mainly from irradiation deformation. This spring relaxation, along with grid growth and fuel rod creep down, results in increased clearance between the fuel rod and the grid support [65]. The altered spring to fuel rod loading combined with flow-induced excitation forces can then lead to relative motion between the fuel rod and grid support, leading to wear damage.

With this spacer design, an example of a potential fuel fret mark is shown in Figure 2-3; this mark developed in a laboratory test simulating flow conditions and resulted from contact with a grid cell dimple. The depths of these marks ranged from 50 μm up to 80 μm. A simple and conservative evaluation of the effect these marks have on the stress is just to reduce the wall thickness of the corroded cladding by the depth of the fret mark. Thus the maximum hoop stress is now 83 MPa based on a local wall thickness of 0.41 mm (initial full wall thickness was 0.57 mm). An axial profile through the maximum depth region of a fret mark of depth 60 μm is shown in Figure 2-4. One might then expect the locations of maximum risk to be the sharp radii at the corners of the fret mark, “A” in Figure 2-4. An estimate of the consequences of such stress concentrations is to raise the axial stress from 42 MPa up to about 95 MPa [66].

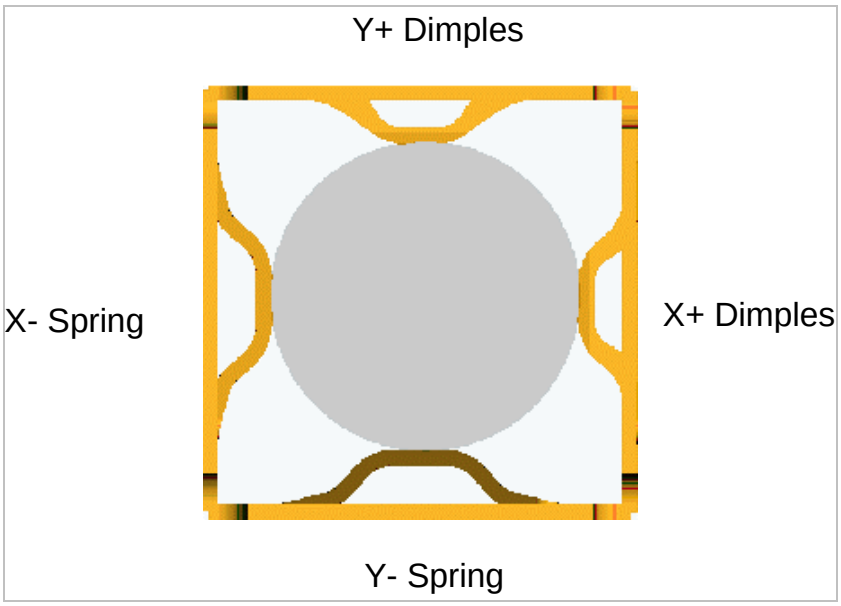

Figure 2-2
Example of PWR fuel rod and grid cell arrangement [63]

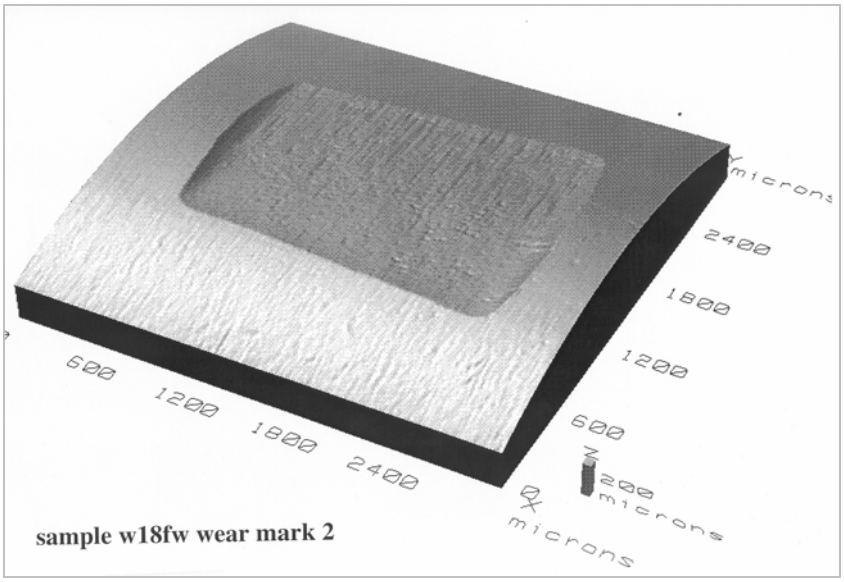

Figure 2-3
Profilometry scan of a fuel rod wear mark resulting from contact with a grid cell dimple during an autoclave fretting-wear test [63]

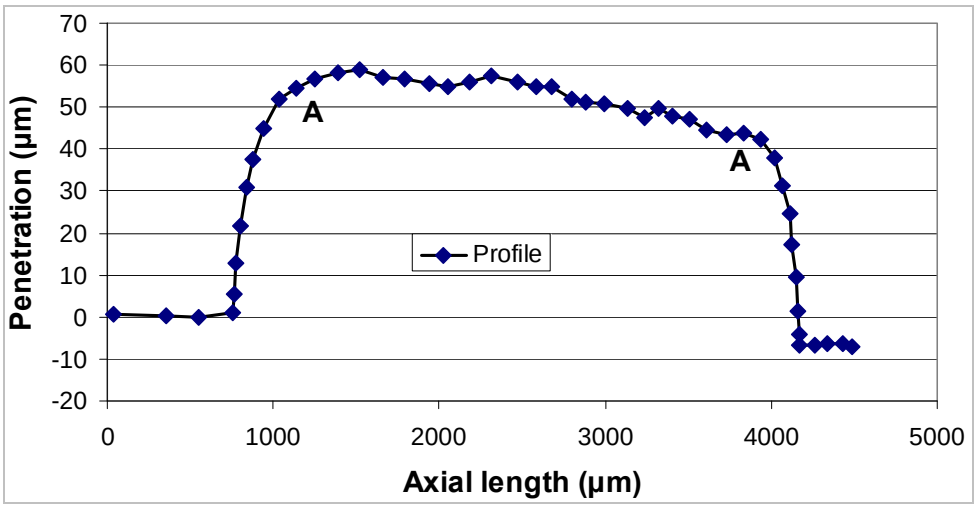

Figure 2-4
Axial profile through the deepest part of a typical fret mark formed during an autoclave fretting-wear test

2.4 Prospects for DHC during Pool Storage

2.4.1 General Considerations

The great decrease in the internal pressure by cooling the fuel in a water pool much reduces the chance of DHC. Applying the analysis used in Section 1 shows that for DHC to start the flaw must be very large and through the wall of the cladding. For a crack to be initiated, the combination of tensile stress and flaw size must exceed K_{IH}. The maximum depth of sharp surface flaw, a, that can be tolerated without crack growth can be estimated from Equation 1-3:

$$a = (K_{IH}/\sigma)^2 \, Q/(1.2\,\pi) \qquad \text{Equation 2-1}$$

where σ = Applied stress
Q = Shape factor

For semi-elliptical flaws, Q is about 1.5 while for long flaws, for example, a scratch, Q is about 1.0. Some estimates are summarized in Table 2-2. For a sharp flaw 25 % through the reduced wall to propagate:

- The hoop stresses have to be very large (310 or 255 MPa in Table 2-2); there is no source of such stresses in spent fuel stored in a water pool, or
- K_{IH} has to be very low (1.3 or 1.6 MPa√m in Table 2-2); there is no evidence for such small values.

Table 2-2
Critical flaw depth for crack initiation by DHC (Wall thickness taken at fret mark as 0.41 mm)

Crack shape depth/length	Q/(1.21 π)	K_{IH} [MPa√m]	Tensile stress [MPa]	Flaw depth [mm]	Flaw depth/Wall thickness
0.3	0.39	5	83	1.43	3.49
0.3	0.39	5	310	0.10	0.25
0.3	0.39	1.3	83	0.10	0.25
0.3	0.39	5	133	0.56	1.36
< 0.1	0.26	5	83	0.95	2.33
< 0.1	0.26	5	255	0.10	0.25
< 0.1	0.26	1.6	83	0.10	0.25
<0.1	0.26	5	133	0.37	0.91

These results suggest that flaws that could propagate by DHC would be detected before the fuel was placed in storage or that DHC will be absent during pool storage of intact fuel. The maximum hoop stress of 83 MPa developed in the fret marks being considered here is far from any stress required to initiate DHC from a smooth surface – 450 MPa in Zr-2.5Nb - again suggesting that the fret marks, although undesirable, should not lead to DHC. The stress concentrating radii at the bottom of a fret mark augment the axial stress. Fuel cladding usually has a very strong radial texture with very few basal plane normals in the axial direction. If fuel cladding behaves in the same way as pressure tubes, which also have very few basal plane normals and high K_{IH} in the axial direction, then DHC would not be initiated at these sharp radii.

2.4.2 Penetration Time

In the unlikely event that DHC was initiated during pool storage, how long would it take to penetrate the fuel cladding? The time for a crack to extend a set distance has two components: the time for the crack to initiate and the time for the crack to grow the distance through the cladding wall. The latter can be estimated from the crack growth rates. The envelope of cases is indicated in Table 2-3, ranging from full wall thickness to that diminished by corrosion and fretting, and using extrapolated crack growth rates, assuming an increase from irradiation. All the times are much shorter than the expected residence times in a storage pool, ranging from 293 days down to 21 days. Any propagating crack would have had sufficient time to cause leakage of radioactivity but none has been documented from this mechanism, further emphasizing that DHC is not an active mechanism during pool storage of fuel.

Table 2-3
Time taken to penetrate fuel cladding by DHC after a crack has been nucleated

Material	Wall thickness [mm]	Crack growth rate [m/s]	Time to penetrate wall [days]
Unirradiated	0.57	2.25×10^{-11}	293
Three times increase in V by irradiation	0.57	6.75×10^{-11}	98
Ten times increase in V by irradiation	0.57	2.25×10^{-10}	29
Unirradiated	0.41	2.25×10^{-11}	211
Three times increase in V by irradiation	0.41	6.75×10^{-11}	70
Ten times increase in V by irradiation	0.41	2.25×10^{-10}	21

Crack initiation times cannot be estimated when the stressing conditions are less than K_{IH} or its equivalent in tensile stress. Even when the stresses are large, setting up the conditions for DHC can take years. As an example, during the installation of the Zr-2.5Nb pressure tubes in the Bruce CANDU reactors very large residual tensile stresses, up to 620 MPa, were set up at the ends of many fuel channels. Once the consequences of these stresses were discovered – cracking and leakage through the tubes [6] – the ends of the pressure tubes in the Bruce units were stress-relieved. The times between installation and stress relief differed between units; the temperature during this interval was about 25 °C. In Unit 1 the stress relief was done 22 months after installation and no cracks formed whereas in Unit 2 the tubes were stress relieved 32 months after installation and four tubes cracked. Although the tensile stresses were very large in Unit 1, no DHC was initiated in almost two years. The stress conditions in fuel cladding during pool storage are much less severe so the expectation would be for very long crack initiation times.

2.4.3 Leaving the Pool

The chief change for the fuel when it is transferred to dry storage is for the temperature to rise. Consequently the internal gas pressure will also increase. The susceptibility to DHC will not change because K_{IH} is temperature insensitive up to at least 250 °C. If the temperature rise is monotonic towards its maximum value, >300 °C, any crack will stop at about 230 °C because of the effect of heating on DHC (T_3 in Figure 1-5 in Section 1). Thus if any incipient crack does not crack before 230 °C is reached, the discussion in Section 1 applies at higher temperatures, again suggesting that DHC is unlikely. The stress at this temperature in the fret mark will rise to 133 MPa but the size of the critical crack would be still be very large, Table 2-2.

2.5 Summary and Conclusions

The features of delayed hydride crack in zirconium alloys and the conditions of spent nuclear fuel at temperatures appropriate for pool storage have been outlined. One potential source of defects is fretting; analysis of fuel rod fretting in a modern grid arrangement suggests that either the stress or the defect sizes are not available to initiate DHC. As with dry storage, DHC is most unlikely during pool storage and during transfer to dry storage.

Section 3: References

[1] INTERNATIONAL ATOMIC ENERGY AGENCY, Survey of wet and dry spent fuel storage, IAEA-TEC-DOC 1100, Vienna, (1999).

[2] WASYWICH, K.M., FREIRE-CANOSA, J., NAQVI, S.J., Canadian spent fuel storage experience, International Symposium on Safety and Engineering Aspects of Spent Fuel Storage, Vienna, October 1994, International Atomic Energy Agency, (1995), 41-55.

[3] RASHID, Y.R., SUNDERLAND, D.J., MONTGOMERY, R.O., Creep as the limiting mechanism for spent fuel dry storage, EPRI Report 1001207, Palo Alto, CA, (2000).

[4] Canadian Standards Association, Technical requirements for in-service evaluation of zirconium alloy pressure tubes in CANDU reactors, N285.8-05, (2005).

[5] KIM, Y.S., Driving force for delayed hydride cracking of zirconium alloys, Metals and Materials International, 11, (2005), 29-38.

[6] PERRYMAN, E.C.W., Pickering pressure tube cracking experience, Nucl. Energy, 17, (1978), 95-105.

[7] SIMPSON, C.J., ELLS, C.E., Delayed hydrogen embrittlement in Zr-2.5wt%Nb, J. Nucl. Mater., 52, (1974), 289-295.

[8] COLEMAN, C.E., et al., Mitigation of harmful effects of welds in zirconium alloy components, Zirconium in the Nuclear Industry – Tenth International Symposium, ASTM STP 1245, A.M. Garde and E.R. Bradley, Eds., American Society for Testing and Materials, Philadelphia, (1994), 264-284.

[9] RESTA LEVI, M., PULS, M.P., DHC behaviour of irradiated Zr-2.5Nb pressure tubes up to 365°C, 18th Inter. Conf. Structural Mechanics in Reactor Technology, (2005), Paper G10-3.

[10] SAGAT, S., COLEMAN, C.E., GRIFFITHS, M., WILKINS, B.J.S., Effect of fluence and irradiation temperature on delayed hydride cracking in Zr-2.5Nb, Zirconium in the Nuclear Industry – Tenth International Symposium, ASTM STP1245, A.M. Garde and E.R. Bradley, Eds.,

American Society for Testing and Materials, Philadelphia, PA., (1994), 35-61.

[11] CHEADLE, B.A., COLEMAN, C.E., AMBLER, J.F.R., Prevention of delayed hydride cracking in zirconium alloys, ASTM STP 939, Zirconium in the Nuclear Industry – Seventh International Symposium", R.B. Adamson and L.F.P. Van Swam, Eds., American Society for Testing and Materials, Philadelphia, PA., (1987), 224-240.

[12] SAGAT, S., CHOW, C.K., PULS, M.P., COLEMAN, C.E., Delayed hydride cracking in zirconium alloys in a temperature gradient, J. Nucl. Mater., 279, (2000), 107-117.

[13] SMITH, R.R., EADIE, R.L., High temperature limit for delayed hydride cracking, Scripta Met., 22, (1988), 833-836.

[14] PAN, Z.L., et al., Effect of irradiation on the fracture properties of Zr-2.5Nb pressure tubes at the end of design life, J.ASTM International, 2, (2005), Paper JAI 12436 (Also see ASTM STP 1467, (2006), 759-782).

[15] COLEMAN, C.E., INOZEMTSEV, V.V., Measurement of Rates of Delayed Hydride Cracking (DHC) in Zr-2.5 Nb alloys – an IAEA Coordinated Research Project, J. ASTM International, 5, (2008), Paper ID JAI101091.

[16] COLEMAN, C.E., et al., Delayed hydride cracking in Zircaloy fuel cladding – an IAEA Coordinated Research Programme, Nucl. Eng. Tech., 41, (2009), 171-178.

[17] PULS, M.P., SIMPSON, L.A., DUTTON, R., Hydride-induced crack growth in zirconium alloys, AECL Report, AECL-7392, (1982).

[18] HUANG, F.H., MILLS, W.J., Delayed hydride cracking behavior for Zircaloy-2 tubing, Met. Trans., 22A, (1991), 2049-2060.

[19] EFSING, P., PETTERSSON, K., The Influence of temperature and yield strength on delayed hydride cracking in hydrided Zircaloy-2, Zirconium in the Nuclear Industry: Eleventh International Symposium, ASTM STP 1295, (1996), 394-404.

[20] GRIGORIEV, V., JAKOBSSON, R., Delayed hydrogen cracking velocity and J-Integral measurements on irradiated BWR cladding, Zirconium in the Nuclear Industry: Fourteenth International Symposium, ASTM STP 1467, (2006), 711-728.

[21] EFSING, P., PETTERSSON, K., Delayed Hydride Cracking in irradiated Zircaloy cladding, Zirconium in the Nuclear Industry: Twelfth International Symposium, ASTM STP 1354, (2000), 340-355.

[22] SCHOFIELD, J.S., DARBY, E.C., GEE, C.F., Temperature and hydrogen concentration limits delayed hydride cracking in irradiated Zircaloy, Zirconium in the Nuclear Industry – Thirteenth International Symposium, ASTM STP 1423, G. D. Moan and P. Rudling, Eds., American Society for Testing and Materials, West Conshohocken, PA., (2002), 339-357.

[23] GRIGORIEV, V., Data presented at Workshop for Studsvik Cladding Integrity Project (SCIP), 2009 November 17.

[24] SAKAMOTO, K., NAKATSUKA, M., HIGUCHI, T., ITO, K., Role of radial temperature gradients in outside-in type failure of high burn-up fuel cladding tubes during power ramp tests, Proc. Top Fuel 2009, Paris, France, (2009), Paper 2076.

[25] SCHRIRE, D., et al., Secondary Defect Behaviour in ABB BWR Fuel, Proc. International Topical Meeting on Light Water Reactor Fuel Performance, West Palm Beach, ANS, (1994), 398-409.

[26] EDSINGER, K., A Review of Fuel Degradation in BWRs, Proc. International Topical Meeting on Light Water Reactor Fuel Performance, Park City, USA, ANS, (2000), 162-179.

[27] SHIMADA, S., ETOH, E., HAYASHI, H., TUKUTA, Y., A metallographic and fractographic study of outside-in cracking caused by power ramp test, J. Nucl. Mater., 327, (2004), 97-113.

[28] SAKAMOTO, K., NAKATSUKA, M., HIGUCHI, T., Simulation of cracking during outside-in type failure of high burn-up fuel cladding tubes, Water Reactor Fuel Performance Meeting, Seoul, Korea, (2008), paper 8009.

[29] UNNIKRISHNAN, K., et al., Observation of delayed hydride cracking in PHWR fuel assembly, 10th CNS International Conference on CANDU Fuel, Ottawa, Canada, (2008).

[30] HIGGY, H. R., HAMMAD, F. H., Effect of neutron irradiation on the tensile properties of Zircaloy-2 and Zircaloy-4, J. Nucl. Mater., 44, (1972), 215-227.

[31] ONCHI, T., KAYANO, H., HIGASHIGUCHI, Y., The inhomogeneous deformation behaviour of neutron irradiated Zircaloy-2, J. Nucl. Mater., 88, (1980), 226-235.

[32] REGNARD, C., VERHAEGHE, B., LEFEBVRE-JOUD, F., LEMAIGNAN, C., Activated slip systems and localized straining of irradiated alloys in circumferential loadings, Zirconium in the Nuclear Industry – Thirteenth International Symposium, ASTM STP 1423, G. D. Moan and P. Rudling, Eds., American Society for Testing and Materials, West Conshohocken, PA., (2002), 384-399.

[33] TORIMARU, T., YASUDA, T., NAKATSUKA, M., Changes in mechanical properties of irradiated Zircaloy-2 fuel cladding due to short term annealing, J. Nucl. Mater., 238, (1996), 169-174.

[34] RIBIS, J., et al., Experimental and modeling approach of irradiation defects recovery in zirconium alloys: impact of an applied stress, J. ASTM International, 5, (2008), Paper ID JAI101118.

[35] LEDERGERBER, G., LIMBÄCK, M., ABOLHASSANI, S., Characterisation of high burn-up fuel irradiated in KKL, Water Reactor Fuel Performance Meeting, Kyoto, Japan, (2005), 396-402.

[36] SELL, H-J., TRAPP-PRITSCHING, S., GARZAROLLI, F., Effect of alloying elements and impurities on in-BWR corrosion of Zirconium alloys, J.ASTM International, 3, (2006), Paper ID JAI12372.

[37] MIYASHITA, T., et al., Corrosion and hydrogen pick-up behaviors of cladding and structural components in BWR high burn-up 9x9 lead use assemblies, LWR Fuel Performance/ TopFuel Meeting, San Francisco, CA., (2007), 401-408.

[38] TSUKUDA, Y., et al., Performance of advanced fuel materials for high burn-up, ENS TopFuel, Nuclear Fuel for Today and Tomorrow: Experience and Outlook, Würzburg, Germany, 16-19 March (2003).

[39] BURTON, H.H., Hydrogen effects on Zircaloy-2 tensile properties, USAEC report HW-61077, (1959).

[40] ARSENE, S., BAI, J.B, BOMPARD, P., Hydride embrittlement and irradiation effects on the hoop mechanical properties of pressurized water reactor (PWR) and boiling water reactor (BWR) Zircaloy cladding tubes: Part 1. Hydride embrittlement in stress-relieved, annealed, and recrystallized Zircaloys at 20°C and 300°C, Met. Mat. Trans., 33A, (2003), 553- 566.

[41] MARSHALL, R.P., LOUTHAN, M.R., Tensile properties of Zircaloy with oriented hydrides, Trans. ASM, 56, (1963), 693-700.

[42] AOMI, M., et al., Evaluation of hydride reorientation behavior and mechanical properties for high-burnup fuel-cladding tubes in interim dry storage, J. ASTM International, 5, (2008), Paper ID JAI101262.

[43] COLEMAN, C.E., Effect of texture on hydride reorientation and delayed hydrogen cracking in cold-worked Zr-2.5 Nb, Zirconium in the Nuclear Industry – Fifth International Symposium, ASTM STP 754, D.G. Franklin, Ed., American Society for Testing and Materials, Philadelphia, PA., (1982), 393-411.

[44] GARDE, A.M., SMITH, G.P., PIREK, R.C., Effects of hydride precipitation localization and neutron fluence on the ductility of irradiated

Zircaloy-4, Zirconium in the Nuclear Industry: Eleventh International Symposium, ASTM STP 1295, (1996), 407-430.

[45] DAUM, R.S., MAJUMDAR, S., BILLONE, M.C., Experimental and analytical investigation of the mechanical behavior of high-burnup Zircaloy-4 fuel cladding, J. ASTM International, 5, (2008), Paper ID JAI101209.

[46] SCHRIRE, D., Personal communication, 2009 November.

[47] PIRON, J., PELLETIER, M., Spent nuclear fuel evolution in a closed system, Eighth Int. Conf., Radioactive Waste Management and Environmental Remediation, ICEM 2001, Bruges, Belgium, (2001).

[48] BRACH, E.W., Cladding consideration for the transportation and storage of spent fuel, USNRC Interim Staff Guidance – 11, Revision 3, Spent Fuel Project Office, (2003).

[49] GOLL, W., LEGER, A.-C., MCCOY, K., Spent fuel behavior under dry cask storage conditions, ANS/ENS TopFuel Conference, Wurzburg, Germany, (2003).

[50] SPILKER, H., PEEHS, M., DYCK, H-P., KASPAR, G., NISSAN, K., Spent LWR fuel dry storage in large transport and storage casks after extended burnup, J. Nucl. Mater., 250, (1997), 63-74.

[51] RASHID, J., MACHIELS, A., Threat of hydride re-orientation to spent fuel integrity during transportation accidents: myth or reality? Proc. Inter. LWR Fuel Performance Meeting, San Francisco, CA, (2007), paper 1039.

[52] EINZIGER, R.E., TSAI, H., BILLONE, M.C., HILTON, B.A., Examination of spent pressurized water reactor fuel rods after 15 years in dry storage, Nucl. Tech., 144, (2003), 186-200.

[53] SASAHARA, A., MATSUMURA, T., Post-irradiation examinations focused on fuel integrity of spent BWR-MOX and PWR-UO_2 fuels stored for 20 years, Nucl. Eng. Design, 238, (2008), 1250-1259.

[54] TIFFANY, C.F., MASTERS, J.N., in Fracture Toughness Testing and its Applications, ASTM STP 381, American Society for Testing and Materials, (1965), 249-277.

[55] MOAN, G.D., et al., Leak-before-break in the pressure tubes of CANDU reactors, Int. J. Pres.Ves. and Piping, 43, (1990), 1-21.

[56] COLEMAN, C.E., AMBLER, J.F.R., Susceptibility of Zr alloys to delayed hydrogen cracking, Zirconium in the Nuclear Industry, ASTM STP 633, A.L. Lowe, Jr. and G.W. Parry, Eds., American Society for Testing and Materials, Philadelphia, PA., (1977), 589-607.

[57] SIMPSON, L.A., NUTTALL, K., Factors controlling hydrogen assisted subcritical crack growth in Zr-2.5 Nb alloys, Zirconium in the Nuclear Industry, ASTM STP 633, A.L. Lowe, Jr. and G.W. Parry, Eds., American Society for Testing and Materials, Philadelphia, PA., (1977), 608-629.

[58] SIMPSON, L.A., PULS, M.P., The effects of stress, temperature and hydrogen content on hydride-induced crack growth in Zr-2.5 pct.Nb, Met. Trans., 10A, (1979), 1093-1105.

[59] COLEMAN, C.E., et al., The effect of microstructure on delayed hydride cracking behavior of Zircaloy-4 fuel cladding – an International Atomic Energy Agency Coordinated Research Program, J. ASTM Inter., 7, (2010), Paper ID JAI103008.

[60] RODGERS, D.K., Private communication, Chalk River Laboratories, (2011).

[61] KANG, K.H., RYU, H.J., SONG, K.C., YANG, M.S., Thermal expansion of UO_2 and simulated DUPIC fuel, J. Nucl. Mater., 301, (2002), 242-244.

[62] BUNNELL, L.R., BATES, J.L., MELLINGER, G.B., Some high-temperature properties of Zircaloy-Oxygen alloys, J. Nucl. Mater., 116, (1983), 219-232.

[63] IAEA, Review of fuel failures in water-cooled reactors, Nuclear Energy Series No. NF-T-21, (2010).

[64] KING, S.J., YOUNG, M.Y., GUÉROUT, F.M., FISHER, N.J., Fretting-Wear Behavior of Zircaloy-4, OPTIN, and ZIRLO Fuel Rods and Grid Supports Under Various Autoclave and Hydraulic Loop Endurance Test Conditions, J. ASTM International, 2, (2005). Paper ID JAI12438.

[65] WEST, J.P., et al., "Challenges for the Nuclear Fuel – A Utility Perspective", An international Topical Meeting on Light Water Reactor Fuel Performance, American Nuclear Society, Park City, UT, 2000.

[66] LEITCH, B.W., Private communication, Chalk River Laboratories, (2011).

Appendix A:Models for DHC Rates

A.1 Introduction

Recently a controversy has arisen over the rate-controlling process for DHC propagation. In a series of papers, starting with [A.1], Y.S. Kim has proposed a model for the rate of DHC that is claimed to be new and superior to previous models. The source of the technical disagreement is in the development of the first step of the process:

- In Kim's model, a hydride is said to precipitate at a crack tip immediately on the imposition of a tensile stress; this model will be called the **P**recipitate **F**irst **M**odel (PFM). Hydrogen diffuses down the concentration gradient set up at the crack tip.
- In an alternative model, the hydrogen moves to the crack tip as a result of the chemical potential gradient set up by the stress gradient at the crack tip. If the increased hydrogen concentration exceeds the solubility limit for precipitation, hydrides are formed. If $K_I > K_{IH}$, the hydride can crack and the process is repeated at the new crack tip. DHC has started. This model will be called the **D**iffusion **F**irst **M**odel (DFM). This model is described in detail in [A.2]. It is a formal presentation of an old idea, using some of the features of the original model by Dutton and Puls [A.3].

A.2 Kim's Model

The essence of the PFM is illustrated in Figure A-1. When a compact tension specimen of zirconium alloy containing 60 ppm hydrogen and a fatigue-sharpened crack is heated beyond 310 °C (point A) all the hydrogen is in solution. On cooling to 250 °C, the hydrogen is still all in solution (point B); Kim says it is supersaturated with respect to the TSSD line, point C. The amount of supersaturation corresponds to BC. When the tensile stress is applied to the specimen, the work energy available from the applied tensile stress will compensate for part of the increased lattice strain energy by precipitating hydrides that have a 14 to 17 % larger volume than the zirconium lattice. Nucleation of hydride only at the crack tip is triggered by the application of tensile stress. The supersaturated hydrogen concentration in the zirconium matrix close to the crack tip is lowered, eventually to the TSSD, point C. The bulk of the specimen is still at point B, and the maximum difference in hydrogen concentration, Δc, between the crack tip and the bulk material is BC. It is Δc that is said to be the driving force for DHC, moving hydrogen down a concentration

gradient from the bulk to the crack tip. The method by which one leaps from this picture to a value of crack growth rate is absent.

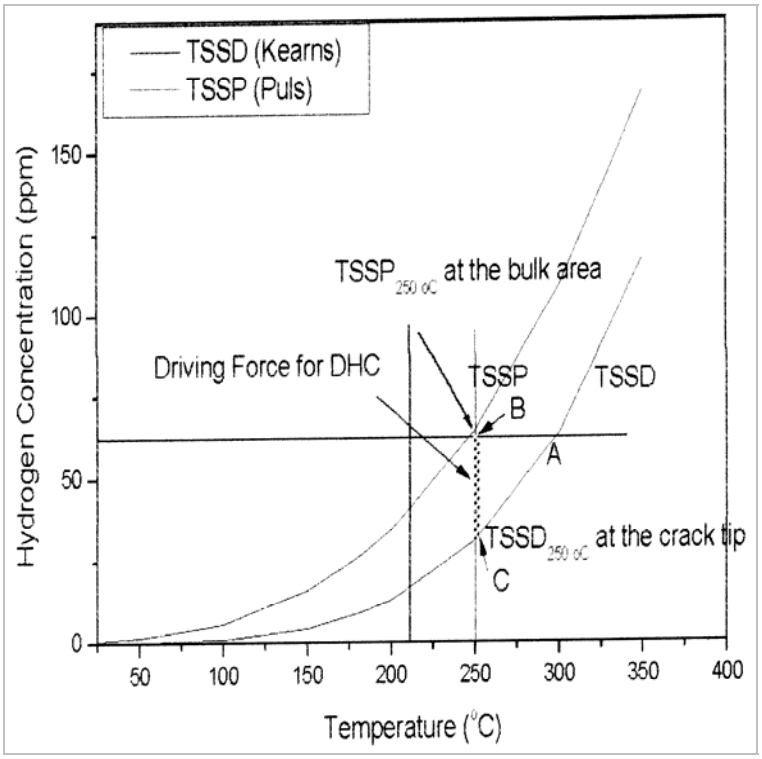

Figure A-1
Schematic diagram of Kim's model (from [A.1])

Problems with this model and its presentation are:

It requires TSSP to be affected by stress. No experimental evidence exists to support this requirement. Theoretical analysis using the experimentally determined partial molar volume of hydrogen in zirconium, V_H, [A.4, A.5] shows that any effect of tensile stress on the solvi is very small [A.6].

It requires that the region between TSSP and TSSD be considered supersaturation.

The size of the concentration gradient is not spelled out. A concentration gradient has the units Mass/(Length)^4, which is not a force.

No analysis leading to equations that can be tested quantitatively against data are provided. Support for this picture of the mechanism is claimed based on correlations.

A.3 DFM

In this model the hydrogen is driven by a gradient in chemical potential, μ, (which does have the units of a force: (Mass x Length)/(Time)^2). This gradient arises because a tensile stress reduces μ [A.7] and at a stress riser μ is lower than in the bulk material. Hydrogen will flow to the region of greatest tensile stress to

compensate for the gradient in μ, that is, from the bulk to the crack tip. Equilibrium is reached when the gradient in μ is zero; consequently the flux of hydrogen stops. A consequence of the hydrogen flow is a concentration gradient, with the concentration being higher at the crack tip than in the bulk (the exact opposite to Kim's PFM once he has precipitated an initial hydride). If the hydrogen concentration at the crack tip reaches TSSP before it reaches the equilibrium concentration, hydrides will form at the crack tip. Further, if $K_I > K_{IH}$, DHC can start. Cracking is not an equilibrium process so hydrogen continues to diffuse to the crack. The equivalent to Kim's picture for DFM is illustrated in Figure A-2 using a loaded compact tension specimen of zirconium alloy containing 60 ppm hydrogen and a fatigue-sharpened crack. The specimen is heated to 340 °C so all the hydrogen is in solution. The concentration of hydrogen in the bulk material, C(b), is 60 ppm while the tensile stress at the crack tip increases the concentration in solution, C(a), to 87 ppm through:

$$C(a) = C(b)\exp[(\mu^0(b)-\mu^0(a)]/RT \qquad \textit{Equation A-1}$$

where $\mu^0(b) - \mu 0(a) = -\sigma_H V_H$, and σ_H is the hydrostatic stress and V_H is the partial molar volume of hydrogen in zirconium.

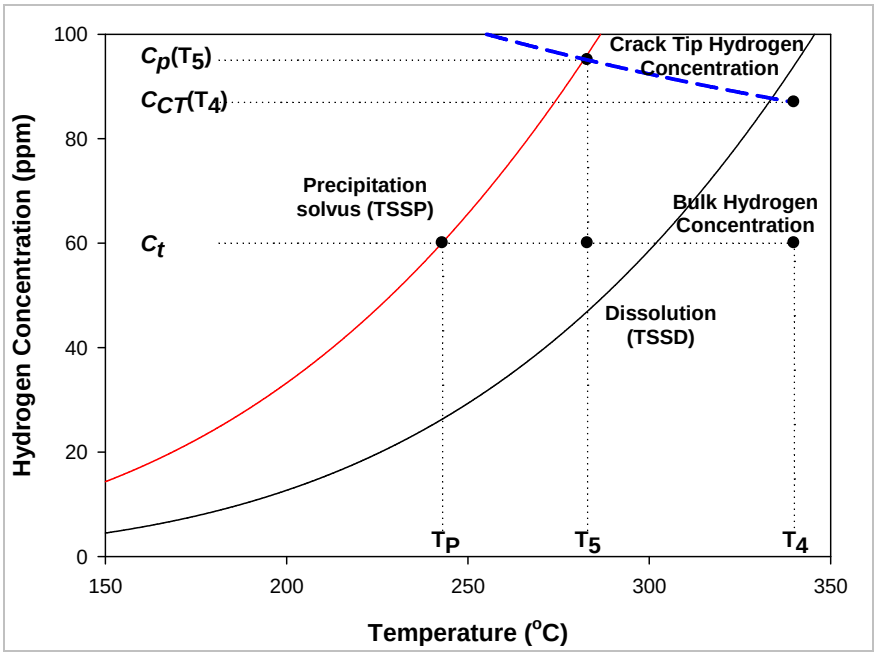

Figure A-2
Schematic diagram of DFM. The critical temperature for DHC is T5 [A.2]

The volume of material around the crack tip is so much smaller than the bulk material that its concentration is assumed to be unaffected by any increase in concentration at the crack tip. Thus on cooling, the concentration in the bulk remains at 60 ppm while that at the crack tip increases because the yield stress is increasing, following equilibrium – the dashed line in Figure A-2. As the TSSD line is crossed at 302 °C, the hydrogen concentration at the crack tip increases to 92 ppm, which is below TSSP. At T_5 (283 °C), TSSP is reached at the crack tip

as its concentration increases to 95 ppm. The crack tip hydrogen concentration in solution cannot exceed TSSP (that would be supersaturation) and hydrides can now precipitate. These hydrides could crack if $K_I > K_{IH}$. Note that T_5 is 40 °C above the TSSP temperature for 60 ppm hydrogen, so no hydrides are present in the bulk in this example. Much experimental evidence is available to support this behavior, Figure A-3.

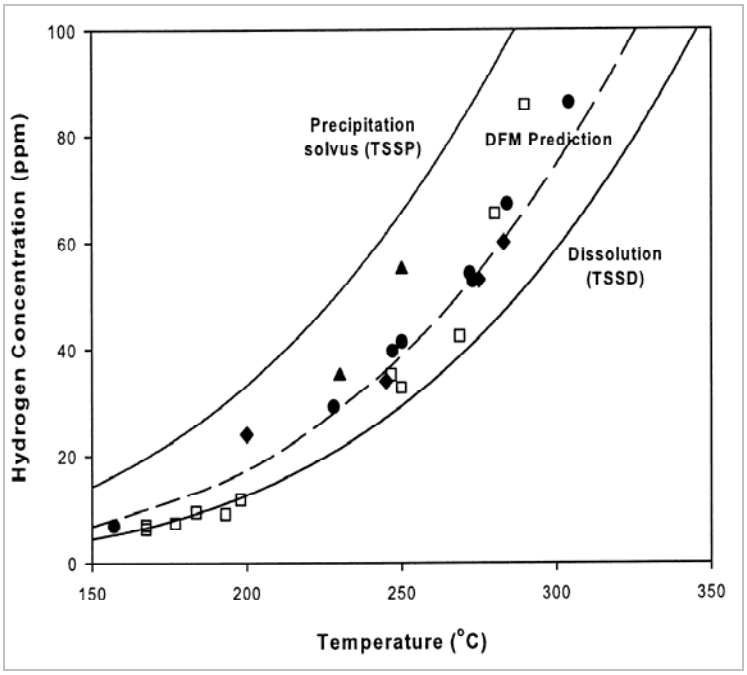

Figure A-3
Measurement of temperature at which DHC can start on cooling, following the scheme of Figure A-2. Data from Zr-2.5Nb (open squares, triangles and circles) and irradiated Zircaloy (diamonds). The dashed line is the DFM prediction (from [A.2])

Since cracking of the hydride is a rapid process, the rate of growth of the hydride and its cracking are controlled by the diffusion of hydrogen into the crack tip. The rate of cracking, V, was derived using this model:

$$V = W D [C_b - C_P \exp(-\sigma_H V_H / RT)] \qquad \text{Equation A-2}$$

where W = Constant,
D = Diffusivity
C_b = Concentration of hydrogen in the bulk material.
C_P = TSSP,
σ_H = Hydrostatic stress; $2.4\sigma_y$ for plane strain and $1.3\ \sigma_y$ for plane stress, and σ_y is the temperature-dependent yield strength.

This model has accurately and quantitatively described several sets of measurements of crack velocity with a range of temperature histories. For example, the results of an international inter-laboratory study [A.8] were

analyzed. The Zr-2.5Nb compact tension specimens contained hydrogen concentrations ranging from 29 to 72 ppm. Before loading, the specimens were heated to beyond TSSD. They were loaded at various temperatures ranging from 144 to 283 ºC; the specimens with the highest hydrogen concentrations were tested at temperatures above TSSP. The test data were accurately described by the DFM, Figure A-4. An exception was found at the lowest test temperature. The open circles all represent calculations based on a TSSP for δ-hydride. The open square at 1000/T = 2.4 is based on a TSSP representing γ-hydride. Although one may invoke a stress-induced phase transformation [A.9], this single point suggests that cracking of γ- and δ-precipitates can be analyzed by DFM simply on the basis of their respective solubility limits.

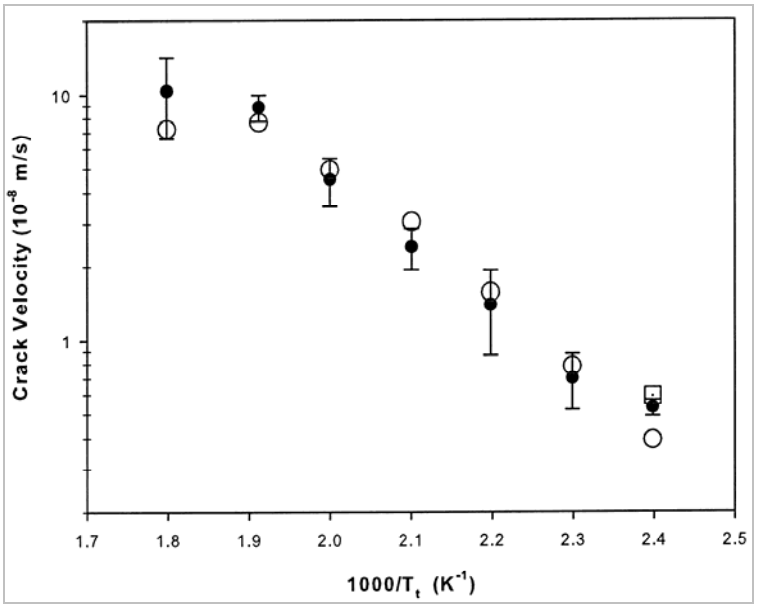

Figure A-4
DFM description (open circles) of the temperature dependence of DHC velocity in Zr-2.5Nb (from [A.2]).

A.4 Discussion

Both models require diffusion of hydrogen to the crack tip, thus separating them quantitatively is difficult. For example, in Section 3.4 of [A.2] an attempt is made to place Kim's model on a mathematical footing; both DFM and PFM described the data. Both require stress to effect change, but in quite different ways: PFM based on stress-induced precipitation and DFM based on stress-induced diffusion. Neither model provides a fracture criterion; if the rate of hydrogen diffusing to the crack tip is the rate controlling process then no fracture criterion is required to describe the rate of crack growth. Because of this silence, these models cannot be used to evaluate K_{IH}, the key to whether cracking can be initiated during dry storage. By extension, Kim is not justified in using his model to describe dry storage [A.10]. His citing of the failures in Zr-2.5Nb fuel cladding at room temperature [A.11] is inappropriate because the cracking was initiated by very large internal stresses created by welding. The hoop stresses

during dry storage will be at least three times smaller than those developed in Zr-2.5Nb after welding.

The impetus for the development of Kim's picture was the perceived shortcomings of the previous approaches.

1. *Hydrogen does not move up a stress gradient.* In experiments with a small stress gradient (12 MPa/mm) no hydrogen transfer from low to high stress regions was detected [A.12]. However, in experiments where the stress gradient was increased by about a factor of 18, at 300 ºC a concentration gradient of about 2 ppm H/mm was detected [A.5]. This result illustrates the small size of the effect and explains why no hydrogen gradient was detected with the low stress gradient. The results in [A.5] were used to calculate the partial molar volume of hydrogen in solution in zirconium, V_H. A value of 1.7×10^{-6} m^3/mol was obtained, which is very close to the value obtained by measurement of the crystal lattice expansion caused by hydrogen in solution [A.4].
2. *If the material contains hydrogen at the solubility limit for dissolution, TSSD, the hydrogen concentration at the crack tip cannot be raised by a stress gradient to attain the solubility limit for hydride precipitation, TSSP, therefore no cracking occurs because no hydrides form.* This statement is true, but as was shown by Figure A-3, this criticism is misplaced and inappropriate because in the DFM, the critical temperature for cracking to start has nothing to do with TSSD.
3. *If the hydrogen concentration reaches TSSP, insufficient hydrogen is available to form a hydride.* This criticism belies the definition of the solubility limit.
4. *A mechanism based on a stress gradient cannot predict the temperature dependence of DHC.* The examples given in [A.2] clearly demonstrate that the DFM describes several sets of data, including the effects of temperature cycling.
5. *A mechanism based on a stress gradient cannot rationalize the low dependence of DHC velocity on K_I.* The elastic stress distribution at a crack tip is limited by plastic deformation. As a crack grows, K_I increases but the stress distribution at the crack tip does not change. Since the DFM depends on this stress distribution, the predicted rates are independent of K_I.

A.5 Conclusions

Two models for the rate of DHC have been briefly described. The PFM advocated by Kim has several technical difficulties and is not well enough analyzed to provide quantitative predictions, despite the many publications. The DFM is a robust, quantitatively verified model based on well-known thermodynamics requiring no unrealistic assumptions, just well-characterized variables such as the solubility limit for hydride precipitation, yield strength, diffusivity and partial molar volume of hydrogen in zirconium.

A.6 References

[A.1] KIM, Y.S., Driving force for delayed hydride cracking of zirconium alloys, Metals and Materials International, 11, (2005), 29-38.

[A.2] McRAE, G.A., COLEMAN, C.E., LEITCH, B.W., The first step for delayed hydride cracking in zirconium alloys, J. Nucl. Mater., 396, (2010), 130-143.

[A.3] DUTTON, R., PULS, M.P., A theoretical model for hydrogen induced sub-critical crack growth, Proc. Effect of Hydrogen on Behavior of Materials, A.W. Thompson and I.M. Bernstein, Eds., Metal Society, AIME, New York, (1976), 516-528.

[A.4] MACEWEN, S.R., COLEMAN, C.E., ELLS, C.E. FABER, J.JR., Dilation of h.c.p. zirconium by interstitial deuterium, Acta Met., 33, (1985), 753-757.

[A.5] EADIE, R.L., TASHIRO, K., HARRINGTON, D., LEGER, M., The determination of the partial molar volume of hydrogen in zirconium in a simple stress gradient using comparative microcalorimetry, Scripta Met. et Mat., 26, (1992), 231-236.

[A.6] PULS, M.P., LEITCH, B.W., SHI, S-Q., The effect of applied stress on the accommodation energy and the solvi for the formation and dissolution of zirconium hydride, Hydrogen Effects on Material Behaviour and Corrosion Deformation Interactions, N.R. Moody et al., eds., The Minerals, Metals and Materials Soc., (2003),233-248.

[A.7] LI, J.C.M., ORIANI, R.A., DARKEN, L.S., The thermodynamics of stressed solids, Z. Physik Chem. Neue Folge, 49, (1966), 271-279.

[A.8] COLEMAN, C.E., INOZEMTSEV, V.V., Measurement of Rates of Delayed Hydride Cracking (DHC) in Zr-2.5 Nb alloys – an IAEA Coordinated Research Project, J. ASTM International, 5, (2008), Paper ID JAI101091.

[A.9] STEUWER, A., SANTISTEBAN, J.R., PREUSS, M., PEEL, M.J., BUSLAPS, T., HARADA, M., Evidence of stress-induced hydrogen ordering in zirconium hydrides, Acta Mat., 57, (2009), 145-152.

[A.10] KIM, Y.S., Delayed hydride cracking of spent fuel rods in dry storage, J. Nucl. Mater., 378, (2008), 30-34.

[A.11] SIMPSON, C.J., ELLS, C.E., Delayed hydrogen embrittlement in Zr-2.5wt%Nb, J. Nucl. Mater., 52, (1974), 289-295.

[A.12] KAMMENZIND, B.F., BERQUIST, B.M., BAJAJ, R., KREYNS, P.H., FRANKLIN, D.G., The long-range migration of hydrogen through Zircaloy in response to tensile and compressive stress gradients,

Zirconium in the Nuclear Industry: Twelfth International Symposium, ASTM STP 1354, (2000), 196-233.

WARNING: This Document contains information classified under U.S. Export Control regulations as restricted from export outside the United States. You are under an obligation to ensure that you have a legal right to obtain access to this information and to ensure that you obtain an export license prior to any re-export of this information. Special restrictions apply to access by anyone that is not a United States citizen or a permanent United States resident. For further information regarding your obligations, please see the information contained below in the section titled "Export Control Restrictions."

Export Control Restrictions

Access to and use of EPRI Intellectual Property is granted with the specific understanding and requirement that responsibility for ensuring full compliance with all applicable U.S. and foreign export laws and regulations is being undertaken by you and your company. This includes an obligation to ensure that any individual receiving access hereunder who is not a U.S. citizen or permanent U.S. resident is permitted access under applicable U.S. and foreign export laws and regulations. In the event you are uncertain whether you or your company may lawfully obtain access to this EPRI Intellectual Property, you acknowledge that it is your obligation to consult with your company's legal counsel to determine whether this access is lawful. Although EPRI may make available on a case-by-case basis an informal assessment of the applicable U.S. export classification for specific EPRI Intellectual Property, you and your company acknowledge that this assessment is solely for informational purposes and not for reliance purposes. You and your company acknowledge that it is still the obligation of you and your company to make your own assessment of the applicable U.S. export classification and ensure compliance accordingly. You and your company understand and acknowledge your obligations to make a prompt report to EPRI and the appropriate authorities regarding any access to or use of EPRI Intellectual Property hereunder that may be in violation of applicable U.S. or foreign export laws or regulations.

The Electric Power Research Institute Inc., (EPRI, www.epri.com) conducts research and development relating to the generation, delivery and use of electricity for the benefit of the public. An independent, nonprofit organization, EPRI brings together its scientists and engineers as well as experts from academia and industry to help address challenges in electricity, including reliability, efficiency, health, safety and the environment. EPRI also provides technology, policy and economic analyses to drive long-range research and development planning, and supports research in emerging technologies. EPRI's members represent more than 90 percent of the electricity generated and delivered in the United States, and international participation extends to 40 countries. EPRI's principal offices and laboratories are located in Palo Alto, Calif.; Charlotte, N.C.; Knoxville, Tenn.; and Lenox, Mass.

Together...Shaping the Future of Electricity

Programs:

Nuclear Power

Used Fuel and High-Level Waste Management

1022921

Electric Power Research Institute
3420 Hillview Avenue, Palo Alto, California 94304-1338 • PO Box 10412, Palo Alto, California 94303-0813 USA
800.313.3774 • 650.855.2121 • askepri@epri.com • www.epri.com